J. Fluid Mech. (2020), *vol.* 888, A11. © The Author(s), 2020.
Published by Cambridge University Press
doi:10.1017/jfm.2020.32

Boundary layer formulations in orthogonal curvilinear coordinates for flow over wind-generated surface waves

Kianoosh Yousefi[1,2,†] **and Fabrice Veron**[2]

[1]Department of Mechanical Engineering, University of Delaware, Newark, DE 19716, USA

[2]School of Marine Science and Policy, University of Delaware, Newark, DE 19716, USA

(Received 11 June 2019; revised 20 September 2019; accepted 9 December 2019)

The development of the governing equations for fluid flow in a surface-following coordinate system is essential to investigate the fluid flow near an interface deformed by propagating waves. In this paper, the governing equations of fluid flow, including conservation of mass, momentum and energy balance, are derived in an orthogonal curvilinear coordinate system relevant to surface water waves. All equations are further decomposed to extract mean, wave-induced and turbulent components. The complete transformed equations include explicit extra geometric terms. For example, turbulent stress and production terms include the effects of coordinate curvature on the structure of fluid flow. Furthermore, the governing equations of motion were further simplified by considering the flow over periodic quasi-linear surface waves wherein the wavelength of the disturbance is large compared to the wave amplitude. The quasi-linear analysis is employed to express the boundary layer equations in the orthogonal wave-following curvilinear coordinates with the corresponding decomposed equations for the mean, wave and turbulent fields. Finally, the vorticity equations are also derived in the orthogonal curvilinear coordinates in order to express the corresponding velocity–vorticity formulations. The equations developed in this paper proved to be useful in the analysis and interpretation of experimental data of fluid flow over wind-generated surface waves. Experimental results are presented in a companion paper.

Key words: surface gravity waves, wind–wave interactions, wave–turbulence interactions

1. Introduction

The investigation of shear flows with streamline curvature are generally challenging problems in fluid mechanics with various applications in engineering and science. Boundary layer flows, in particular, are strongly affected by even a mild surface curvature through the production of additional rates of strain (Bradshaw 1973). Although the effects of curvature on turbulent flows over convex and concave solid and fixed surfaces with a mild curvature have been extensively investigated

† Email address for correspondence: kyousefi@udel.edu

theoretically (e.g., Bradshaw 1969; So 1975; Hall & Horseman 1991; Holloway & Tavoularis 1998), experimentally (e.g., So & Mellor 1973; Ramaprian & Shivaprasad 1978, 1982; Hoffmann *et al.* 1985; Barlow & Johnston 1988; Holloway & Tavoularis 1992; Holloway *et al.* 2005), and numerically (e.g., Moser & Moin 1987; Neves *et al.* 1994; Kim & Rhode 2000; Blin *et al.* 2003; Dave *et al.* 2013) over the past decades, there exist substantially fewer studies of the flow in the boundary layer over liquid, propagating surface waves (e.g., Takeuchi *et al.* 1977; Hsu *et al.* 1981; Hsu & Hsu 1983; Sullivan *et al.* 2000; Yang & Shen 2010; Buckley & Veron 2016). Thus, the current understanding of airflow over surface waves, for example, remains hampered by the complexities associated with the geometrical shape of surface waves. It is observed, in general, that the surface curvature not only changes the mean velocity profiles but also exerts considerable influences on the fluctuation velocity components, shear stress, and turbulent stress compared to similar flows over flat surfaces.

To capture these effects of curvature on the structure of the fluid flow, it is practical to express the governing equations of motion in general orthogonal or non-orthogonal coordinates. Indeed, the additional production, convection, and diffusion terms due to the curvature of flow appear explicitly in those kinds of coordinate systems (Bradshaw 1973; Moser & Moin 1987). One way to transform the equations of motion from rectangular coordinates to the general coordinates is to transform the coordinate system but not the dependent flow variables such as velocity components. That is, the rectangular flow field is interpreted in a curvilinear coordinate system. For the study of water waves, for example, this approach has been employed by Hsu *et al.* (1981), Hsu & Hsu (1983), Sullivan *et al.* (2000), Shen *et al.* (2003), Yang & Shen (2010, 2017), Druzhinin *et al.* (2016), and Yang *et al.* (2018), among others, and it yields relatively simple equations where the results can be readily interpreted. Moreover, the experimental realizations, particularly single-point measurements, can be performed quite easily (Hsu *et al.* 1981). Another approach is to completely transform the coordinate system along with the dependent flow variables into the curvilinear coordinate system such that the dependent variables, for example, the velocity components are aligned with the axes of the new coordinate system (e.g., Gent & Taylor 1976; Al-Zanaidi & Hui 1984; Shyu & Phillips 1990; Longuet-Higgins 1998). While this kind of transformation simplifies the theoretical analysis as well as numerical modelling, it is generally impractical for conducting experiments (Hsu *et al.* 1981). It should also be pointed out that although the non-orthogonal coordinates are frequently employed in the simulations of airflow over waves (e.g., Sullivan *et al.* 2008; Yang & Shen 2010; Hara & Sullivan 2015; Xuan *et al.* 2019; Hao & Shen 2019) mainly due to convenience in grid generation, they introduce additional complexities in the governing equations. These complexities are primarily associated with the presence of the covariant and contravariant velocity components that leads to different forms of the governing equations. Furthermore, the general curvilinear non-orthogonal coordinates give rise to extra metric tensors, and besides that, the fields in the conservation equations might not have their usual physical meanings (see Richmond *et al.* 1986; Finnigan 2004). The governing equations are, however, significantly more straightforward in the orthogonal coordinate systems and preserve much of the analytical simplicity of their counterpart equations in the Cartesian coordinates. The main reason is that no distinction between covariant and contravariant vector and tensor fields exists for the orthogonal coordinate systems.

In the study of ocean surface waves, the wave-coherent motion poses serious challenges to the full transformation of the problem where the separation of mean, wave, and turbulent is required for a complete treatment of the wave-turbulence interaction (Einaudi & Finnigan 1993). The triple decomposition of flow field variables into mean, wave, and turbulent components was first introduced by Hussain & Reynolds (1972) and has been extensively applied to air-sea interaction studies. A great number of these numerical and experimental studies, however, are carried in a fixed Cartesian frame of reference (e.g., Finnigan & Einaudi 1981; Einaudi & Finnigan 1993; Mastenbroek *et al.* 1996; Makin & Kudryavtsev 1999; Hara & Belcher 2004; Rutgersson &

Sullivan 2005). In such coordinate systems, the wave-associated motions cannot be captured below the highest wave crest (Sullivan *et al.* 2000; Hara & Sullivan 2015), thereby demonstrating the importance of employing a wave-following coordinate system. It should also be noted here that while recent computational studies now routinely employ the algebraic mapping to investigate the wave-induced motions very close to the surface and to address difficulties associated with the non-rectangular physical domain over surface waves, experimental studies have just begun to report such data using wave-following coordinate systems (e.g., Buckley & Veron 2016, 2017).

Air-sea interaction studies investigating fluid flow, including continuity, momentum, and kinetic energy equations along with the corresponding triple-decomposed equations in a general coordinate system are extremely sparse. Gent & Taylor (1976) expressed the conventional Reynolds decomposed continuity, momentum, and turbulent energy equations in a wave-following curvilinear coordinate system proposed by Benjamin (1959) in order to numerically investigate the two-dimensional (2D) flow field in a turbulent boundary layer over water waves. The mean governing equations were then closed by the use of an isotropic eddy viscosity model. The equations of 2D turbulent fluid motion were also derived for an orthogonal streamline coordinate system by Finnigan (1983). It was shown that the transformed mean equations for the first and second moments of velocity involve explicit extra terms representing the influences of streamline curvature and the acceleration of the mean flow. These Reynolds decomposed equations were also expressed by Kantha & Rosati (1990) in generalized orthogonal curvilinear coordinates to study the influence of streamline curvature on small-scale turbulence. The algebraic transformation of the governing equations into a surface-fitted curvilinear coordinate system has been widely employed in computational studies of surface waves over the past decades. In order to investigate the turbulent flow over water waves, a 2D conformal and orthogonal transformation was used by Sullivan *et al.* (2000) to map the physical domain on to a computational grid, and consequently, transform only the coordinates in the governing equations into a surface-fitted, orthogonal coordinate system. To examine the wind-wave interaction in the marine boundary layer, Sullivan *et al.* (2008) expressed the 2D large-eddy simulation (LES) equations including mass conservation, momentum, and energy transport equations in a non-orthogonal, hybrid rectangular-curvilinear computational coordinate system through introducing the contravariant flux velocities (see also Sullivan *et al.* 2000, 2014). The ensemble-averaged equations for the momentum and energy budgets are further derived by Sullivan *et al.* (2018) in similar hybrid computational coordinates where the vertical lines are held fixed while the horizontal axis is wave-following.

A comprehensive analysis of the wave boundary layer turbulence over surface waves in a strongly forced condition was carried out recently by Hara & Sullivan (2015). In their study, the dynamical governing equations along with the corresponding mean, wave, and turbulent equations were derived in a hybrid, wave-following coordinate system similar to the one used by Sullivan *et al.* (2014) and Sullivan *et al.* (2018). The triple decomposition formulations in wave-following coordinates define the expression for the wave-induced stress as a sum of the wave and pressure stresses compared to the traditional definition (e.g., Makin & Kudryavtsev 1999; Hara & Belcher 2004) in terms of the wave-coherent velocity components. Finally, there are some recent attempts to express the viscous tangential stresses at the air-water interface in an orthogonal wave-following coordinate system (see Buckley & Veron 2017; Iafrati *et al.* 2019), but we note that these estimates are valid only in the linear wave limit.

In the study of turbulent flows over propagating surface waves, the necessity of employing a wave-following coordinate system has been recognized (e.g., Hsu *et al.* 1981; Sullivan *et al.* 2000; Hara & Sullivan 2015), and therefore, as mentioned above, the algebraic mapping of rectangular coordinates into wave-following coordinates has commonly been employed in theoretical and numerical studies, and just recently, in laboratory measurements. However, the further step of fully transforming the governing equations with the dependent flow variables into those coordinate

systems is rarely taken, and to the best of the authors' knowledge, the decomposed mean, wave, and turbulent equations required for the complete treatment of wave-turbulence interaction are not yet fully derived. This is in part due to the mathematical difficulties associated with the curvilinear coordinates and the fact that experimental studies have not been able to estimate the additional geometric terms appearing in the transformed equations. In the current study, therefore, we present the fully-transformed governing equations of fluid flow including continuity, momentum, and kinetic energy equations in the wave-following orthogonal curvilinear coordinate system along with the triple-decomposed form of those equations. The orthogonal general coordinate system is physically intuitive and appropriate for the study of the turbulent flow over surface waves since it can provide an alternative framework in which the surface-parallel continuity, momentum, and energy budget equations can be thoroughly investigated which leads to a better physical interpretation of many quantities in the governing equations. The complete transformation of the governing equations also directly allows us to account for the streamline curvature. Finally, we simplify the equations for the mean, wave, and turbulent fields using classical boundary layer approximations. The fluid flow governing equations in orthogonal curvilinear coordinates are presented in § 2, and the corresponding triple-decomposed equations are expressed in § 3. We narrow our focus to the weakly non-linear waves in § 4 and perform a boundary layer scaling. The triple-decomposed equations for the boundary layer are then derived in § 4.1. We finally offer a brief conclusion in § 5. The § Appendix A provides the velocity-vorticity formulations in orthogonal curvilinear coordinates. Analysis of experimental data using the framework developed in this paper are presented in a companion paper (Yousefi *et al.* 2019).

2. Fluid flow governing equations

The governing equations of fluid motion, including continuity, momentum, and kinetic energy equations in a turbulent flow are first derived in an orthogonal curvilinear coordinate system. These equations are then decomposed into mean, wave-induced, and turbulence components by employing the triple decomposition technique. To express the equations of motion, the flow is assumed to have a constant density, a constant kinematic viscosity, and velocity components $\boldsymbol{u} = (u_1, u_2, u_3)$ in x_1, x_2, and x_3 directions, respectively. The continuity, momentum, and energy equations for an incompressible fluid can be written in an invariant vector form as,

$$\boldsymbol{\nabla} \cdot \boldsymbol{u} = 0 \tag{2.1}$$

$$\rho \frac{\partial \boldsymbol{u}}{\partial t} + \rho \left(\boldsymbol{u} \cdot \boldsymbol{\nabla}\right) \boldsymbol{u} = -\boldsymbol{\nabla} p + \boldsymbol{\nabla} \cdot \boldsymbol{\tau} \tag{2.2}$$

$$\rho \frac{\partial e}{\partial t} + \rho \left(\boldsymbol{\nabla} \cdot e\boldsymbol{u}\right) = -\boldsymbol{\nabla} \cdot (p\boldsymbol{u}) + (\boldsymbol{\nabla} \cdot \boldsymbol{\tau}) \cdot \boldsymbol{u} \tag{2.3}$$

where $\boldsymbol{u}$ is the velocity vector, ρ is the density, and p is the pressure which includes the static gravity term gz. Also $\boldsymbol{\tau} = 2\mu \boldsymbol{S}$ is the viscous stress tensor, μ is the dynamic viscosity, $2\boldsymbol{S} = (\boldsymbol{\nabla u} + (\boldsymbol{\nabla u})^T)$ is the strain rate tensor, and $e = (\boldsymbol{u} \cdot \boldsymbol{u})/2$ is the kinetic energy. The velocity gradient tensor is noted $\boldsymbol{\nabla u}$ and $(\boldsymbol{\nabla u})^T$ is its transpose.

2.1. *Orthogonal curvilinear coordinates*

Fixed rectangular coordinate systems are not able to capture the effects of streamline curvature, and particularly in the study of wind waves, no spatially or temporally averaged information can be obtained beneath the highest wave crest (e.g., Sullivan *et al.* 2000; Hara & Sullivan 2015). In order to investigate the wave-induced motions near the interface and/or below the wave crest, it is

thus necessary to employ a coordinate system that closely follows the wave shapes. For example, Hara & Sullivan (2015) and Yang & Shen (2017) have recently employed a coordinate system that follows the vertical displacement due to the surface waves. However, we find that the strictly orthogonal curvilinear coordinate system is practical and physically intuitive. In this section, we derive the continuity, momentum, and energy equations in an orthogonal curvilinear coordinate system.

Let $x_i = (x_1, x_2, x_3)$ represent the Cartesian coordinate system and $\xi_i = (\xi_1, \xi_2, \xi_3)$ represent a set of an arbitrary orthogonal curvilinear coordinates. It is well understood that the distinction between covariant and contravariant components in general non-orthogonal curvilinear coordinates vanishes in orthogonal curvilinear coordinate systems. The orthogonal coordinate basis can then be defined as (Vinokur 1974; Redzic 2001; Shikhmurzaev & Sisoev 2017),

$$\boldsymbol{\xi}_i = \frac{\partial x_k}{\partial \xi_i} \hat{\boldsymbol{e}}_k \tag{2.4}$$

where $\hat{\boldsymbol{e}}_k$ are the corresponding Cartesian orthonormal basis. The base vectors in orthogonal curvilinear coordinates are not necessarily unit vectors. The orthonormal base vectors in orthogonal curvilinear coordinates can be obtained by,

$$\hat{\boldsymbol{\xi}}_i = \frac{\boldsymbol{\xi}_i}{h_i} \tag{2.5}$$

where the quantities h_i are the so-called *scale factors* of the orthogonal curvilinear coordinate system given by,

$$\begin{aligned}
(h_1)^2 &= \left(\frac{\partial x_1}{\partial \xi_1}\right)^2 + \left(\frac{\partial x_2}{\partial \xi_1}\right)^2 + \left(\frac{\partial x_3}{\partial \xi_1}\right)^2 \\
(h_2)^2 &= \left(\frac{\partial x_1}{\partial \xi_2}\right)^2 + \left(\frac{\partial x_2}{\partial \xi_2}\right)^2 + \left(\frac{\partial x_3}{\partial \xi_2}\right)^2 \\
(h_3)^2 &= \left(\frac{\partial x_1}{\partial \xi_3}\right)^2 + \left(\frac{\partial x_2}{\partial \xi_3}\right)^2 + \left(\frac{\partial x_3}{\partial \xi_3}\right)^2
\end{aligned} \tag{2.6}$$

In order to express equations (2.1) to (2.3) in orthogonal curvilinear coordinates, we will first spell out the differential vector operators including gradient, divergence, curl, and Laplacian in orthogonal coordinates. These operators are fairly standard and can be found in the literature (e.g., Aris 1962; Batchelor 1967; Anderson *et al.* 1984; Redzic 2001; Nikitin 2006), but we choose to include them here for completeness. Furthermore, in order to substantially simplify the notation in the remainder of this paper, we propose a notation that builds on and modifies the standard Einstein summation convention. Indeed, throughout this work the index notation is such that *no summing is carried whenever the indices are enclosed within parentheses*. Accordingly, the indices within parentheses only take the value of dummy or free indexes. All other aspects of the summation convention remain unchanged; any index that is repeated twice in any term of expression is called a dummy or repeated index to be summed over the range of its values and any index not repeated is called free index taking any value in its range. For instance, the suffix (i) in the following expression only takes the value of free index i, i.e. $u_i u_j \kappa_{(i)j} = u_1 u_1 \kappa_{11} + u_1 u_2 \kappa_{12} + u_1 u_3 \kappa_{13}$, and the suffix (j) in the following expression takes the value of dummy index j, i.e. $u_j u_j \kappa_{(j)i} = u_1 u_1 \kappa_{1i} + u_2 u_2 \kappa_{2i} + u_3 u_3 \kappa_{3i}$. With this notation, the standard vector and tensor operators can be then expressed in the orthogonal curvilinear coordinate systems in a way that we find elegant and conveniently compact. If φ is an arbitrary scalar, $\mathbf{A}$ is an arbitrary vector, and $\mathbf{T}$ is an arbitrary tensor field, the expressions for the gradient, divergence, curl, and Laplacian operators in the orthogonal curvilinear coordinates become,

$$\boldsymbol{\nabla}\varphi = \frac{1}{h_{(i)}}\frac{\partial\varphi}{\partial\xi_i}\widehat{\boldsymbol{\xi}}_i \tag{2.7}$$

$$\boldsymbol{\nabla}\cdot\mathbf{A} = \frac{1}{h}\frac{\partial}{\partial\xi_i}\left(\frac{h}{h_{(i)}}a_i\right) \tag{2.8}$$

$$\boldsymbol{\nabla}\times\mathbf{A} = \varepsilon_{ijk}\frac{h_{(i)}}{h}\frac{\partial}{\partial\xi_j}\left(h_{(k)}a_k\right)\widehat{\boldsymbol{\xi}}_i \tag{2.9}$$

$$\nabla^2\varphi = \frac{1}{h}\frac{\partial}{\partial\xi_i}\left(\frac{h}{h_{(i)}h_{(i)}}\frac{\partial\varphi}{\partial\xi_i}\right) \tag{2.10}$$

where $h = h_1h_2h_3$. Furthermore,

$$(\mathbf{A}\cdot\boldsymbol{\nabla})\,\mathbf{B} = \left[\frac{a_j}{h_{(j)}}\frac{\partial b_i}{\partial\xi_j} + \left(a_ib_j\kappa_{(i)j} - a_jb_j\kappa_{(j)i}\right)\right]\widehat{\boldsymbol{\xi}}_i \tag{2.11}$$

$$\boldsymbol{\nabla}\cdot\mathbf{T} = \left[\frac{1}{h}\frac{\partial}{\partial\xi_j}\left(\frac{h}{h_{(j)}}T_{ij}\right) + \left(T_{ij}\kappa_{(i)j} - T_{jj}\kappa_{(j)i}\right)\right]\widehat{\boldsymbol{\xi}}_i \tag{2.12}$$

In the above equations, a_i, b_i, and T_{ij} are respectively the components of the vector $\mathbf{A}$, vector $\mathbf{B}$, and tensor $\mathbf{T}$ defined based on the orthonormal basis, and κ_{ij} are the components of the *curvature matrix* which account for the curvature of the coordinate system and can be defined as,

$$\mathcal{K} = \begin{bmatrix} \frac{1}{h_1h_1}\frac{\partial h_1}{\partial\xi_1} & \frac{1}{h_1h_2}\frac{\partial h_1}{\partial\xi_2} & \frac{1}{h_1h_3}\frac{\partial h_1}{\partial\xi_3} \\ \frac{1}{h_1h_2}\frac{\partial h_2}{\partial\xi_1} & \frac{1}{h_2h_2}\frac{\partial h_2}{\partial\xi_2} & \frac{1}{h_2h_3}\frac{\partial h_2}{\partial\xi_3} \\ \frac{1}{h_3h_1}\frac{\partial h_3}{\partial\xi_1} & \frac{1}{h_2h_3}\frac{\partial h_3}{\partial\xi_2} & \frac{1}{h_3h_3}\frac{\partial h_3}{\partial\xi_3} \end{bmatrix} \tag{2.13}$$

Thus, all terms in the continuity, momentum, and energy equations, equations (2.1) through (2.3), can now be expressed in orthogonal curvilinear coordinates. The vector operators presented in equations (2.7) to (2.12) are consistent with those given in the literature by, for example, Aris (1962), Vinokur (1974), Anderson *et al.* (1984), Redzic (2001), and Nikitin (2006) but expressed in a compact and practical form.

2.2. *Continuity, momentum, and energy equations*

In order to express the fluid governing equations, consider arbitrary orthogonal curvilinear coordinates $\xi_i = (\xi_1, \xi_2, \xi_3)$ with corresponding velocity components $\boldsymbol{U} = (U_1, U_2, U_3)$. The velocity components in orthogonal curvilinear coordinates are projections of the velocity vector into the coordinate axes and thus related to the Cartesian velocities by the coordinate transformation. The components of the velocity vector $\boldsymbol{u}$ in both Cartesian and orthogonal curvilinear coordinate systems are schematically illustrated in figure 1. Using the vector operators introduced in equations (2.7) through (2.12), the continuity, momentum, and energy equations can be then written as,

$$\frac{1}{h}\frac{\partial}{\partial\xi_i}\left(\frac{h}{h_{(i)}}U_i\right) = 0 \tag{2.14}$$

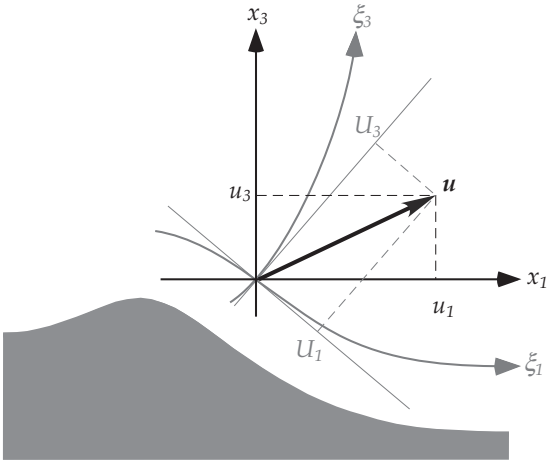

FIGURE 1. Two-dimensional schematics of the velocity components in Cartesian and orthogonal curvilinear coordinate systems. In which, (u_1, u_3) are components of the velocity vector $\boldsymbol{u}$ corresponding to the (x_1, x_3) Cartesian coordinates and (U_1, U_3) are the components of the velocity vector $\boldsymbol{u}$ corresponding to the arbitrary (ξ_1, ξ_3) orthogonal curvilinear coordinates.

$$\frac{\partial U_i}{\partial t} + \frac{U_j}{h_{(j)}}\frac{\partial U_i}{\partial \xi_j} + \left(U_i U_j \kappa_{(i)j} - U_j U_j \kappa_{(j)i}\right) = -\frac{1}{\rho}\frac{1}{h_{(i)}}\frac{\partial p}{\partial \xi_i} + \frac{1}{\rho}\left[\frac{1}{h}\frac{\partial}{\partial \xi_j}\left(\frac{h}{h_{(j)}}\tau_{ij}\right) + \left(\tau_{ij}\kappa_{(i)j} - \tau_{jj}\kappa_{(j)i}\right)\right] \tag{2.15}$$

$$\frac{\partial e}{\partial t} + \frac{U_i}{h_{(i)}}\frac{\partial e}{\partial \xi_i} = -\frac{1}{\rho}\frac{U_i}{h_{(i)}}\frac{\partial p}{\partial \xi_i} + \frac{1}{\rho}\left[\frac{U_i}{h}\frac{\partial}{\partial \xi_j}\left(\frac{h}{h_{(j)}}\tau_{ij}\right) + U_i\left(\tau_{ij}\kappa_{(i)j} - \tau_{jj}\kappa_{(j)i}\right)\right] \tag{2.16}$$

where $e = (U_i U_i)/2$.

Here, it is noted that the governing equations (2.14) to (2.16) are obtained using a time-independent transformation. The continuity, momentum, and energy equations given here for the orthogonal coordinates are quite similar to the conventional Cartesian coordinate system, except for the additional curvature terms that, in fact, account for the curvature of the coordinate system and produced due to the spatial dependence of the base vectors. The Cartesian coordinate equations are simply recovered by noting that $h_i = 1$ for rectangular coordinates. The reader may directly verify that the expanded form of the governing equations (2.14) to (2.16) are identical to the continuity and momentum equations given in the literature for an orthogonal curvilinear coordinate system (e.g., Brown & Hung 1977; Hung & Brown 1977; Raithby *et al.* 1986; Blumberg & Herring 1987; Nikitin 2006; Shen *et al.* 2015).

Again, the viscous stress is,

$$\tau_{ij} = 2\mu S_{ij} \tag{2.17}$$

where the components of the strain rate tensor can now be expressed in an orthogonal coordinate system as,

$$S_{ij} = \frac{1}{2}\left[\frac{1}{h_{(j)}}\frac{\partial U_i}{\partial \xi_j} + \frac{1}{h_{(i)}}\frac{\partial U_j}{\partial \xi_i} - \left(U_{(i)}\kappa_{ij} + U_{(j)}\kappa_{ji}\right) + 2U_m\kappa_{(i)m}\delta_{ij}\right] \tag{2.18}$$

In order to provide a more in-depth explanation of the acceleration and stress terms in equation

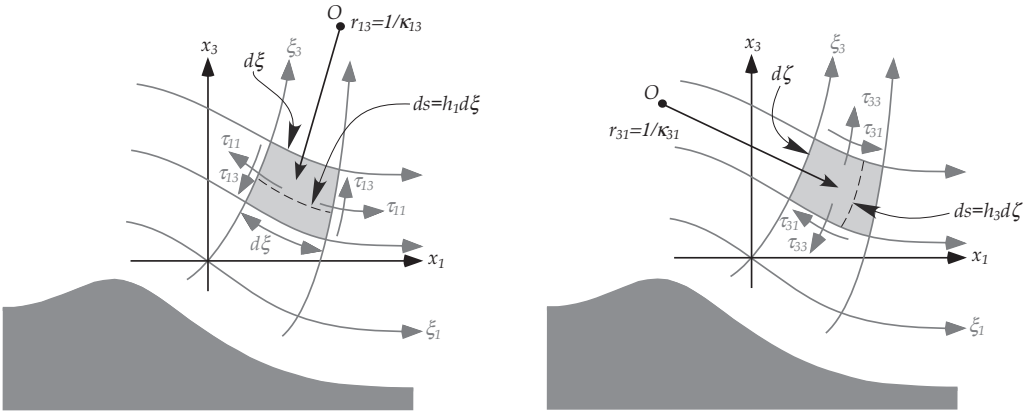

FIGURE 2. Illustration of the viscous stress field along with the curvature parameter in the $\xi_1-\xi_3$ plane of an arbitrary orthogonal curvilinear coordinate system. Here, $r_{31}=1/\kappa_{31}$ and $r_{13}=1/\kappa_{13}$ are the radius of curvature along the constant ξ_1- and ξ_3-coordinate, respectively, with respect to the $\xi_1-\xi_3$ plane. The point where two tangent vectors ξ_1 and $\xi_1+d\xi_1$ intersect is called the centre of curvature and denoted by the point O.

(2.15), which do not traditionally appear in the Cartesian equations, we confine the following discussion to two-dimensional flows in which we neglect the curvature in the lateral direction. The stress components are schematically illustrated along with the curvature parameters in figure 2 in the $\xi_1-\xi_3$ plane of an orthogonal, wave-following coordinate system. The radius of curvature, defined as the reciprocal of the curvature, along the constant ξ_1-coordinate with respect to the $\xi_1-\xi_3$ plane is $r_{31}=1/\kappa_{31}$, whereas the radius of curvature is $r_{13}=1/\kappa_{13}$ along a line of constant ξ_3. Let's rewrite the ξ_1-momentum equation for the two-dimensional steady case described in figure 2, as,

$$\frac{U_1}{h_1}\frac{\partial U_1}{\partial \xi_1}+\frac{U_3}{h_3}\frac{\partial U_1}{\partial \xi_3}+(U_1U_3\kappa_{13}-U_3U_3\kappa_{31})=-\frac{1}{\rho}\frac{1}{h_1}\frac{\partial p}{\partial \xi_1}$$
$$+\frac{1}{\rho}\left[\frac{1}{h}\frac{\partial}{\partial \xi_1}(h_2h_3\tau_{11})+\frac{1}{h}\frac{\partial}{\partial \xi_3}(h_1h_2\tau_{13})+(\tau_{13}\kappa_{13}-\tau_{33}\kappa_{31})\right] \tag{2.19}$$

The contributions of the curvature, or equivalently the radius of curvature, to the fluid-particle acceleration components appears as additional terms. For example $(U_1U_3\kappa_{13}-U_3U_3\kappa_{31})$ are due to the curvature of the coordinates in ξ_3 and ξ_1 directions, respectively. As noted by Raithby *et al.* (1986), the additional component $\tau_{13}\kappa_{13}$ in the viscous stress term arises because τ_{13} has a net component in ξ_1 direction as shown in figure 2a. In a similar fashion, the term $\tau_{33}\kappa_{31}$ arises due to the fact that τ_{33} stresses are seen to have a net component in the negative ξ_1 direction (see figure 2b). The interpretation of the momentum equations in the other directions is quite similar to the ξ_1-momentum equation and it is not presented here to keep brevity.

In orthogonal curvilinear coordinates, both the radius of curvature and the centre of curvature are functions of the arc length, and consequently, they vary from point to point. Moreover, at spatial locations where the ξ-coordinate has inflections points, the curvature is zero and the radius of curvature is infinite, i.e. $\kappa_{31}=0$ and $r_{31}=\infty$.

3. Application to surface waves

In the section above, we have reviewed the conservation equations for fluid in motion using an arbitrary orthogonal curvilinear coordinate system. Our interest, however, is to examine the mean,

wave-induced, and turbulent flow on both sides of a wavy interface. Specifically, we are interested in the airflow above surface gravity waves but do not consider waves with large curvatures such as capillary waves. Experimental results of airflow measurements over wind waves will be presented in the accompanying paper (Yousefi *et al.* 2019). We note here that in the derivations above, the curvilinear system does not vary in time. Strictly speaking, this simply means that the wave shape is assumed to remain unchanged as the waves propagate. For monochromatic waves, the flow is thus examined after an initial Galilean transformation in which the Cartesian system is moving with the wave phase speed so that the wave shape becomes steady. In the case of wind waves with a spectrum of wave modes, the peak wave speed can be used for the Galilean transformation (Sullivan *et al.* 2018). In this case, the wave shape is quasi-steady. This restricts the analysis of the flow to time scales that are faster than that over which the wave shape evolves substantially. We expect this to be the case for the airflow over wind waves when the wind speed is larger than the wave phase speed (i.e. wind forced waves). Indeed, based on the wind-wave spectrum (Elfouhaily *et al.* 1997; Mueller & Veron 2009), we estimate that, in the laboratory and for winds ranging from 5 to 25 m s^{-1}, the wave shape remains correlated at 80% for at least 0.7 peak wave period. In the field, after 0.7 peak wave period, the correlation reduces to 70%. Therefore, over times corresponding to a fraction of the peak wave period, the coordinate transformation outlined above (with Galilean transformation using the peak wave speed) holds for wind waves with multiple modes. We note, however, that the water-side flow is likely to evolve on time scales that are comparable or longer than the time scales over which the wave shape changes.

The issue of separating waves and turbulence has long been a recurrent challenge in the study of surface waves (e.g., Hussain & Reynolds 1970; Lumley & Terray 1983; Thais & Magnaudet 1995). Here, in order extract the organized wave-coherent fluctuations in the flow field from the background turbulence, we decompose instantaneous variables into a phase-averaged component, $\langle f \rangle (\boldsymbol{\xi}, t)$, and a turbulent fluctuation component, $f'(\boldsymbol{\xi}, t)$, as (Hussain & Reynolds 1970),

$$f(\boldsymbol{\xi}, t) = \langle f \rangle (\boldsymbol{\xi}, t) + f'(\boldsymbol{\xi}, t) \tag{3.1}$$

The phase averaged quantity is defined as,

$$\langle f \rangle (\boldsymbol{\xi}, t) = \lim_{N \to \infty} \frac{1}{N} \sum_{n=1}^{N} f(\boldsymbol{\xi} + n\lambda, t)$$

where N is the number of realizations and λ is the surface wave wavelength. The phase average is the average of the values of f at a particular phase of the wave. The phase average can be further decomposed into the sum of a mean, $\bar{f}(\boldsymbol{\xi})$, and a wave-induced, $\tilde{f}(\boldsymbol{\xi}, t)$, component, i.e. $\langle f \rangle (\boldsymbol{\xi}, t) = \bar{f}(\boldsymbol{\xi}) + \tilde{f}(\boldsymbol{\xi}, t)$. The mean is defined as the ensemble average over all possible phases. This separation leads to the following so-called triple decomposition of an instantaneous quantity,

$$f(\boldsymbol{\xi}, t) = \bar{f}(\boldsymbol{\xi}) + \tilde{f}(\boldsymbol{\xi}, t) + f'(\boldsymbol{\xi}, t) \tag{3.2}$$

where the wave-induced motion has a zero mean but is phase-coherent with the surface waves and thus not considered turbulent per se. The general properties of the ensemble and phase averages can be found in reports by Hussain & Reynolds (1970), Hussain & Reynolds (1972), and Reynolds & Hussain (1972). The equations of motion including continuity, momentum, and energy for an organized wave in a turbulent shear flow are then derived using this triple decomposition approach.

3.1. *Continuity and momentum equations*

The starting point to derive the decomposed equations is to substitute the decomposed field quantities into the governing equations, and then averaging; the ensemble averaging is applied first and then the phase averaging. For an incompressible fluid, the mean, wave-induced, and

turbulent continuity equations in an orthogonal curvilinear coordinate system can therefore be expressed as,

$$\frac{1}{h}\frac{\partial}{\partial \xi_i}\left(\frac{h}{h_{(i)}}\overline{U}_i\right) = 0 \tag{3.3}$$

$$\frac{1}{h}\frac{\partial}{\partial \xi_i}\left(\frac{h}{h_{(i)}}\widetilde{U}_i\right) = 0 \tag{3.4}$$

$$\frac{1}{h}\frac{\partial}{\partial \xi_i}\left(\frac{h}{h_{(i)}}U_i'\right) = 0 \tag{3.5}$$

Using continuity, the instantaneous momentum equation (2.15) can be written as,

$$\begin{aligned}\frac{\partial U_i}{\partial t} + \frac{1}{h}\frac{\partial}{\partial \xi_j}\left(\frac{h}{h_{(j)}}U_iU_j\right) + \left(U_iU_j\kappa_{(i)j} - U_jU_j\kappa_{(j)i}\right) = -\frac{1}{\rho}\frac{1}{h_{(i)}}\frac{\partial p}{\partial \xi_i} \\ + \frac{1}{\rho}\left[\frac{1}{h}\frac{\partial}{\partial \xi_j}\left(\frac{h}{h_{(j)}}\tau_{ij}\right) + \left(\tau_{ij}\kappa_{(i)j} - \tau_{jj}\kappa_{(j)i}\right)\right]\end{aligned} \tag{3.6}$$

Substituting the decomposed velocity and pressure fields into the momentum equation above (3.6) and then applying ensemble averaging yields the momentum equation for the mean flow,

$$\begin{aligned}\frac{D\overline{U}_i}{Dt} + \frac{1}{h}\frac{\partial}{\partial \xi_j}\left(\frac{h}{h_{(j)}}\overline{\tilde{U}_i\tilde{U}_j}\right) + \left(\overline{\tilde{U}_i\tilde{U}_j}\kappa_{(i)j} - \overline{\tilde{U}_j\tilde{U}_j}\kappa_{(j)i}\right) \\ + \frac{1}{h}\frac{\partial}{\partial \xi_j}\left(\frac{h}{h_{(j)}}\overline{U_i'U_j'}\right) + \left(\overline{U_i'U_j'}\kappa_{(i)j} - \overline{U_j'U_j'}\kappa_{(j)i}\right) \\ = -\frac{1}{\rho}\frac{1}{h_{(i)}}\frac{\partial \bar{p}}{\partial \xi_i} + \frac{1}{\rho}\left[\frac{1}{h}\frac{\partial}{\partial \xi_j}\left(\frac{h}{h_{(j)}}\bar{\tau}_{ij}\right) + \bar{\tau}_{ij}\kappa_{(i)j} - \bar{\tau}_{jj}\kappa_{(j)i}\right]\end{aligned} \tag{3.7}$$

where the ratio of the vertical scale to the principal radius of curvature of the surface is assumed to be small. Also, the mean material derivative defined as,

$$\frac{D}{Dt} = \frac{\partial}{\partial t} + \left(\overline{\mathbf{U}}\cdot\boldsymbol{\nabla}\right) \tag{3.8}$$

and where,

$$\bar{\tau}_{ij} = 2\mu\bar{S}_{ij} = \mu\left[\frac{1}{h_{(j)}}\frac{\partial \overline{U}_i}{\partial \xi_j} + \frac{1}{h_{(i)}}\frac{\partial \overline{U}_j}{\partial \xi_i} - \left(\overline{U}_{(i)}\kappa_{ij} + \overline{U}_{(j)}\kappa_{ji}\right) + 2\overline{U}_m\kappa_{(i)m}\delta_{ij}\right] \tag{3.9}$$

is the mean viscous stress, $\bar{S}_{ij}$ is the mean strain rate tensor, $-\overline{U_i'U_j'}$ is the turbulent stress, and $-\overline{\tilde{U}_i\tilde{U}_j}$ is the wave-induced stress (e.g., Hussain & Reynolds 1972; Hsu *et al.* 1981; Buckley & Veron 2016). The wave-induced stress term evidently makes the mean momentum equation (3.7) different from the conventional Reynolds-averaged equations for the turbulent flows in orthogonal curvilinear coordinate systems (see for example Nash & Patel 1972; Richmond *et al.* 1986; Chen *et al.* 1990). The wave-induced stress is not only significant in the exchange of momentum and energy between the wind and waves particularly in the wave generation process (e.g., Hsu *et al.* 1981; Makin & Mastenbroek 1996) but also is a substantial portion of the total stress close to the surface (e.g., Janssen 1989; Makin *et al.* 1995; Makin & Kudryavtsev 2002). Equations (3.3) and (3.7) together describe the motion of the mean field.

The wave-induced momentum equation can be obtained by applying the phase-averaged

operator to the instantaneous momentum equation (3.6 after substituting the decomposed velocity and pressure terms therein), and substracting the mean momentum equation. The wave-induced momentum equation in an orthogonal curvilinear coordinate system can be therefore expressed as,

$$\begin{aligned}\frac{D\widetilde{U}_i}{Dt}+\frac{1}{h}\frac{\partial}{\partial\xi_j}\left(\frac{h}{h_{(j)}}\overline{U}_i\widetilde{U}_j\right)+\left(\widetilde{U}_i\overline{U}_j\kappa_{(i)j}-\widetilde{U}_j\overline{U}_j\kappa_{(j)i}\right)+\frac{1}{h}\frac{\partial}{\partial\xi_j}\left(\frac{h}{h_{(j)}}\tilde{R}_{ij}\right)\\ +\left(\tilde{R}_{ij}\kappa_{(i)j}-\tilde{R}_{jj}\kappa_{(j)i}\right)+\frac{1}{h}\frac{\partial}{\partial\xi_j}\left(\frac{h}{h_{(j)}}\tilde{r}_{ij}\right)+\left(\tilde{r}_{ij}\kappa_{(i)j}-\tilde{r}_{jj}\kappa_{(j)i}\right)\\ =-\frac{1}{\rho}\frac{1}{h_{(i)}}\frac{\partial\tilde{p}}{\partial\xi_i}+\frac{1}{\rho}\left[\frac{1}{h}\frac{\partial}{\partial\xi_j}\left(\frac{h}{h_{(j)}}\tilde{\tau}_{ij}\right)+\tilde{\tau}_{ij}\kappa_{(i)j}-\tilde{\tau}_{jj}\kappa_{(j)i}\right]\end{aligned} \tag{3.10}$$

where

$$\tilde{\tau}_{ij}=2\mu\tilde{S}_{ij}=\mu\left[\frac{1}{h_{(j)}}\frac{\partial\widetilde{U}_i}{\partial\xi_j}+\frac{1}{h_{(i)}}\frac{\partial\widetilde{U}_j}{\partial\xi_i}-\left(\widetilde{U}_{(i)}\kappa_{ij}+\widetilde{U}_{(j)}\kappa_{ji}\right)+2\widetilde{U}_m\kappa_{(i)m}\delta_{ij}\right] \tag{3.11}$$

is the wave-induced viscous stress, $\tilde{S}_{ij}$ is the wave-induced strain rate tensor, $\tilde{r}_{ij}=\langle U_i'U_j'\rangle-\overline{U_i'U_j'}$ is the wave-induced turbulent stress (e.g., Reynolds & Hussain 1972; Hsu *et al.* 1981; Einaudi *et al.* 1984) which represents the oscillation of the turbulent stress due to the presence of surface waves, and $\tilde{R}_{ij}=\widetilde{U}_i\widetilde{U}_j-\overline{\widetilde{U}_i\widetilde{U}_j}$ is the fluctuating part of the wave stress (e.g., Einaudi *et al.* 1984; Rutgersson & Sullivan 2005). Analogous to wave-induced turbulent stress, $\tilde{R}_{ij}$ can be interpreted as the nonlinear wave contribution to the total fluctuation stress. Moreover, the term $\widetilde{U}_i\widetilde{U}_j$ in the wave-induced wave stress term describes the momentum flux due to wave fluctuations. These terms are of considerable importance in coupling the wave and turbulence fields. Equations (3.4) and (3.10) together describe the wave-induced motion.

In addition to the mean and wave-induced momentum equations, the momentum equation for the background turbulence can also be derived by subtracting equations (3.7) and (3.10) from the decomposed, instantaneous momentum equation. Thus, the momentum equation for the turbulence in an orthogonal general coordinate system is,

$$\begin{aligned}\frac{DU_i'}{Dt}+\frac{1}{h}\frac{\partial}{\partial\xi_j}\left(\frac{h}{h_{(j)}}U_i'\widetilde{U}_j\right)+\left(\widetilde{U}_iU_j'\kappa_{(i)j}-\widetilde{U}_jU_j'\kappa_{(j)i}\right)+\frac{1}{h}\frac{\partial}{\partial\xi_j}\left(\frac{h}{h_{(j)}}\overline{U}_iU_j'\right)\\ +\left(U_i'\overline{U}_j\kappa_{(i)j}-U_j'\overline{U}_j\kappa_{(j)i}\right)+\frac{1}{h}\frac{\partial}{\partial\xi_j}\left(\frac{h}{h_{(j)}}\widetilde{U}_iU_j'\right)\\ +\left(U_i'\widetilde{U}_j\kappa_{(i)j}-U_j'\widetilde{U}_j\kappa_{(j)i}\right)+\frac{1}{h}\frac{\partial}{\partial\xi_j}\left(\frac{h}{h_{(j)}}U_i'U_j'\right)\\ +\left(U_i'U_j'\kappa_{(i)j}-U_j'U_j'\kappa_{(j)i}\right)\\ -\left[\frac{1}{h}\frac{\partial}{\partial\xi_j}\left(\frac{h}{h_{(j)}}\langle U_i'U_j'\rangle\right)+\left(\langle U_i'U_j'\rangle\kappa_{(i)j}-\langle U_j'U_j'\rangle\kappa_{(j)i}\right)\right]\\ =-\frac{1}{\rho}\frac{1}{h_{(i)}}\frac{\partial p'}{\partial\xi_i}+\frac{1}{\rho}\left[\frac{1}{h}\frac{\partial}{\partial\xi_j}\left(\frac{h}{h_{(j)}}\tau_{ij}'\right)+\tau_{ij}'\kappa_{(i)j}-\tau_{jj}'\kappa_{(j)i}\right]\end{aligned} \tag{3.12}$$

where

$$\tau'_{ij} = 2\mu S'_{ij} = \mu\left[\frac{1}{h_{(j)}}\frac{\partial U'_i}{\partial \xi_j} + \frac{1}{h_{(i)}}\frac{\partial U'_j}{\partial \xi_i} - \left(U'_{(i)}\kappa_{ij} + U'_{(j)}\kappa_{ji}\right) + 2U'_m\kappa_{(i)m}\delta_{ij}\right] \tag{3.13}$$

is the turbulent viscous stress and S'_{ij} is the turbulent strain rate tensor. The turbulence of the fluid motion can be then fully expressed by equations (3.5) and (3.12).

3.2. *Mean, wave-induced, and turbulent kinetic energy equations*

In this section, we expand the kinetic energy budget equations and specifically look at the mean, wave-coherent, and turbulent kinetic energy. Following Hussain & Reynolds (1972), Finnigan & Einaudi (1981), and Einaudi & Finnigan (1993), an equation for the *mean kinetic energy budget* can be obtained by multiplying the mean momentum equation (3.7) by $\overline{U}_i$ and then successively phase- and ensemble-averaging,

$$\begin{aligned}\frac{D\bar{e}}{Dt} = \frac{1}{h}\frac{\partial}{\partial \xi_j}\left(-\frac{h}{h_{(j)}}\frac{\bar{p}}{\rho}\overline{U}_j - \frac{h}{h_{(j)}}\overline{U}_i\overline{\tilde{U}_i\tilde{U}_j} - \frac{h}{h_{(j)}}\overline{U}_i\overline{U'_iU'_j} + \frac{h}{h_{(j)}}2\nu\overline{U}_i\bar{S}_{ij}\right)\\ - 2\nu\bar{S}_{ij}\bar{S}_{ij} + \overline{\tilde{U}_i\tilde{U}_j}\bar{S}_{ij} + \overline{U'_iU'_j}\bar{S}_{ij}\end{aligned} \tag{3.14}$$

where $\bar{e} = \overline{U}_i\overline{U}_i/2$ is the mean kinetic energy per unit mass. The left-hand side of this equation describes the rate of change of the mean kinetic energy and the right-hand side represents different mechanisms that precipitate such changes. The first four terms on the right-hand side of equation (3.14) are in flux divergence form, and consequently, describe the spatial transport or redistribution of the mean kinetic energy by the mean pressure, wave perturbations, turbulent stresses, and viscous stresses, respectively. The fifth term $2\nu\bar{S}_{ij}\bar{S}_{ij}$ represents the viscous dissipation of the mean kinetic energy. The last two terms in equation (3.14) are analogous to the well-known shear production term and represent the exchange of energy between the mean flow and the wave-coherent and turbulent fields, respectively. The mean turbulent stress is likely to be positive over the ocean surface waves (e.g., Borue *et al.* 1995; Shen *et al.* 2003; Buckley & Veron 2016), while the mean wave stress is positive below the critical layer and negative above (e.g., Townsend 1972; Hsu *et al.* 1981; Sullivan *et al.* 2000; Yang & Shen 2010). It is also observed that the mean shear is positive over propagating surface waves (e.g., Hara & Sullivan 2015; Husain *et al.* 2019).

The balance of the kinetic energy for the wave-induced motion can be similarly derived by multiplying the wave-induced momentum equation (3.10) with the wave-induced velocity fields and then successively applying the phase- and ensemble-averaged operators,

$$\begin{aligned}\frac{D\bar{\tilde{e}}}{Dt} = \frac{1}{h}\frac{\partial}{\partial \xi_j}\left(-\frac{1}{\rho}\frac{h}{h_{(j)}}\overline{\tilde{p}\tilde{U}_j} - \frac{h}{h_{(j)}}\overline{\tilde{U}_i\tilde{r}_{ij}} - \frac{h}{h_{(j)}}\overline{\tilde{U}_i\tilde{R}_{ij}} + \frac{h}{h_{(j)}}2\nu\overline{\tilde{U}_i\tilde{S}_{ij}}\right)\\ - 2\nu\overline{\tilde{S}_{ij}\tilde{S}_{ij}} - \overline{\tilde{U}_i\tilde{U}_j}\bar{S}_{ij} + \overline{\tilde{R}_{ij}\tilde{S}_{ij}} + \overline{\tilde{r}_{ij}\tilde{S}_{ij}}\end{aligned} \tag{3.15}$$

where $\tilde{e} = \widetilde{U}_i\widetilde{U}_i/2$ is the wave kinetic energy per unit mass and $\bar{\tilde{e}} = \overline{\tilde{U}_i\tilde{U}_i}/2$ is the ensemble-averaged wave kinetic energy. As previous, the left-hand side of equation (3.15) represents the rate of change of the mean kinetic energy, and the right-hand side, representing the transport, production, and dissipation mechanisms producing such changes. The first four terms on the right-hand side of equation (3.15) express the transport of the wave kinetic energy by pressure, wave-induced turbulent stresses, wave-induced wave stresses, and viscous stresses or molecular diffusion. The fifth term, similar to its counterpart in equation (3.14), represents the viscous dissipation rate due to the wave-induced motion. The sixth term is the production term due to the periodic wave which represents the exchanges between mean shear and wave motion. This

term also appears in the mean kinetic energy budget equation (3.14) but with the sign reversed. The last two terms in equation (3.15) are the rate of energy transfer between the wave-induced flow and in turn wave-induced wave stress and wave-induced turbulent stress. These terms are involved in the exchange of kinetic energy between the wave and turbulent fields (see Cheung & Street 1988; Einaudi & Finnigan 1993; Rutgersson & Sullivan 2005). In order to obtain further insights, it should be noticed that the third and seventh terms of the right-hand side of the wave kinetic energy equation can be combined,

$$\frac{1}{h}\frac{\partial}{\partial \xi_j}\left(\frac{h}{h_{(j)}}\overline{\tilde{U}_i \tilde{R}_{ij}}\right) - \overline{\tilde{R}_{ij}\tilde{S}_{ij}} = \frac{1}{h}\frac{\partial}{\partial \xi_j}\left(\frac{h}{h_{(j)}}\overline{\tilde{e}\tilde{u}_j}\right) \tag{3.16}$$

which explicitly describes the transport of the wave kinetic energy by the wave fluctuating part of the total fluctuation stress (Einaudi *et al.* 1984). It is a redistribution term (Rutgersson & Sullivan 2005) that has been usually neglected in previous studies.

Finally, an equation for the balance of the turbulent kinetic energy can be obtained via multiplying the momentum equation for the background turbulence and multiplying by the turbulent velocity and averaging as,

$$\begin{aligned}\frac{D\overline{e'}}{Dt} = {} & \frac{1}{h}\frac{\partial}{\partial \xi_j}\left(-\frac{1}{\rho}\frac{h}{h_{(j)}}\overline{p'U'_j} - \frac{h}{h_{(j)}}\overline{e'U'_j} + \frac{h}{h_{(j)}}2\nu\overline{U'_i S'_{ij}}\right) - 2\nu\overline{S'_{ij}S'_{ij}} - \overline{U'_i U'_j}\bar{S}_{ij} \\ & - \overline{\langle U'_i U'_j\rangle \tilde{S}_{ij}} - \overline{\frac{\tilde{U}_j}{h_{(j)}}\frac{\partial\langle e'\rangle}{\partial \xi_j}}\end{aligned} \tag{3.17}$$

where $e' = U'_i U'_i/2$ is the turbulent kinetic energy per unit mass. Similarly to the mean and wave kinetic energy budgets, the three first terms on the right-hand side of equation (3.17) represent the transport of the turbulent kinetic energy within the flow. They are the pressure transport, the turbulence transport, and viscous diffusion terms, respectively. The fourth term represents the viscous dissipation due to the turbulent motion. The fifth term is the shear production term which describes exchanges between the mean shear and turbulence. This term appears as an energy source term in the mean kinetic energy equation (3.14), but with the opposite sign. The sixth term is the turbulence-wave interaction term (e.g., Rutgersson & Sullivan 2005; Davis & Monismith 2011) describing the turbulent energy production by the waves through the action of the wave-induced turbulent stresses (Reynolds & Hussain 1972; Cheung & Street 1988). This term too is found in the wave kinetic energy equation but with the opposite sign. It is also noticed that $\overline{\langle U'_i U'_j\rangle \tilde{S}_{ij}} = \overline{\tilde{r}_{ij}\tilde{S}_{ij}}$. The last term is the advection of turbulent kinetic energy by waves (e.g., Rutgersson & Sullivan 2005; Tsai *et al.* 2015) and can be expressed as (see, for example, Finnigan & Einaudi 1981),

$$\overline{\frac{\tilde{U}_j}{h_{(j)}}\frac{\partial\langle e'\rangle}{\partial \xi_j}} = \frac{1}{h}\frac{\partial}{\partial \xi_j}\left(\frac{h}{h_{(j)}}\frac{1}{2}\overline{\tilde{r}_{ii}\tilde{U}_j}\right) \tag{3.18}$$

The last two terms on the right-hand side of equation (3.17) describe the interactions between wave and turbulent fields and only appear in a triple-decomposed turbulent kinetic energy equation. The $\overline{U'_i U'_j}\bar{S}_{ij}$, $\overline{\tilde{U}_i\tilde{U}_j}\bar{S}_{ij}$, and $\overline{\tilde{r}_{ij}\tilde{S}_{ij}}$ terms are present in equations (3.14), (3.15), and (3.17), and clearly denote the interaction among the mean, wave, and turbulent fields. Finally, in obtaining equations (3.14) through (3.18), we note that the doubly contracted product of a symmetric tensor with another tensor is equal to the doubly contracted product of the first tensor with the symmetric part of the second tensor (Kundu & Cohen 2002) (because the doubly contracted product of any symmetric tensor with an asymmetric tensor is zero (Boyer & Fabrie 2012)). Therefore, for

example in equation (3.14), $\bar{\boldsymbol{\tau}}_{\text{turb}} : \bar{\mathbf{S}} = \bar{\boldsymbol{\tau}}_{\text{turb}} : \boldsymbol{\nabla}\overline{\mathbf{U}}$ and $\bar{\boldsymbol{\tau}}_{\text{wave}} : \bar{\mathbf{S}} = \bar{\boldsymbol{\tau}}_{\text{wave}} : \boldsymbol{\nabla}\overline{\mathbf{U}}$ where $\bar{\boldsymbol{\tau}}_{\text{turb}}$ is the turbulent stress tensor and $\bar{\boldsymbol{\tau}}_{\text{wave}}$ is the wave stress tensor.

4. Boundary layer scaling

The governing equations of motion, developed in the preceding sections, can be considerably simplified assuming boundary-layer type flows in which the vertical length scale of the motion is small compared to the horizontal length scale. Thus, we are further considering the flow over surface waves wherein the wavelength of the disturbance is large compared to the wave amplitude, i.e. $ak \ll 1$. A non-dimensionalization of the problem described by equations (2.14) to (2.16) is then performed to obtain the reduced form of the equations through identifying the small parameters, after which the resulting equations are made specific for surface waves. To this end, a unified scaling was developed by allowing the vertical scales to be different from horizontal scales. Accordingly, the following set of dimensionless variables, denoted by stars, are introduced,

$$\xi_1^* = k\xi_1, \qquad \xi_2^* = k\xi_2, \qquad \xi_3^* = \frac{\xi_3}{a} \tag{4.1}$$

$$U_1^* = \frac{U_1}{U_{10}}, \qquad U_2^* = \frac{U_2}{U_{10}}, \qquad U_3^* = \frac{U_3}{akU_{10}} \tag{4.2}$$

$$p^* = \frac{p}{\rho U_{10}^2} \tag{4.3}$$

$$t^* = U_{10}kt \tag{4.4}$$

where a is the wave amplitude, k is the wavenumber, ak is the wave slope, and U_{10} is the wind speed measured at 10-m height. It can be noted here that time is non-dimensionalized using the peak frequency as,

$$t^* = \omega t \frac{U_{10}}{c}$$

where c is the phase velocity and U_{10}/c is the inverse of wave age. By substituting the dimensionless variables into the governing equations of an orthogonal curvilinear coordinate system, the resulting non-dimensional equations can be expressed for the continuity,

$$\frac{1}{h}\frac{\partial}{\partial \xi_1^*}\left(\frac{h}{h_1}U_1^*\right) + \frac{1}{h}\frac{\partial}{\partial \xi_2^*}\left(\frac{h}{h_2}U_2^*\right) + \frac{1}{h}\frac{\partial}{\partial \xi_3^*}\left(\frac{h}{h_3}U_3^*\right) = 0 \tag{4.5}$$

and momentum equations,

$$\begin{aligned}
&\frac{\partial U_1^*}{\partial t^*} + \frac{U_1^*}{h_1}\frac{\partial u_1^*}{\partial \xi_1^*} + \frac{U_2^*}{h_2}\frac{\partial U_1^*}{\partial \xi_2^*} + \frac{U_3^*}{h_3}\frac{\partial U_1^*}{\partial \xi_3^*} + U_1^*U_2^*\kappa_{12}^* + U_1^*U_3^*\kappa_{13}^* - U_2^*U_2^*\kappa_{21}^* - \varepsilon^2 U_3^*U_3^*\kappa_{31}^* \\
&\quad = -\frac{1}{h_1}\frac{\partial p^*}{\partial \xi_1^*} + \frac{1}{Re}\left[\frac{1}{h}\frac{\partial}{\partial \xi_1^*}\left(\frac{h}{h_1}\tau_{11}^*\right) + \frac{1}{h}\frac{\partial}{\partial \xi_2^*}\left(\frac{h}{h_2}\tau_{12}^*\right)\right. \\
&\quad + \frac{1}{\varepsilon^2}\frac{1}{h}\frac{\partial}{\partial \xi_3^*}\left(\frac{h}{h_3}\frac{h_1}{h_3}\frac{\partial}{\partial \xi_3^*}\left(\frac{U_1^*}{h_1}\right)\right) + \frac{1}{h}\frac{\partial}{\partial \xi_3^*}\left(\frac{h}{h_3}\frac{h_3}{h_1}\frac{\partial}{\partial \xi_1^*}\left(\frac{U_3^*}{h_3}\right)\right) \\
&\quad \left. + \tau_{12}^*\kappa_{12}^* + \frac{1}{\varepsilon^2}\frac{h_1}{h_3}\frac{\partial}{\partial \xi_3^*}\left(\frac{U_1^*}{h_1}\right)\kappa_{13}^* + \frac{h_3}{h_1}\frac{\partial}{\partial \xi_1^*}\left(\frac{U_3^*}{h_3}\right)\kappa_{13}^* - \tau_{22}^*\kappa_{21}^* - \tau_{33}^*\kappa_{31}^*\right]
\end{aligned} \tag{4.6}$$

$$\begin{aligned}
&\frac{\partial U_2^*}{\partial t^*}+\frac{U_1^*}{h_1}\frac{\partial U_2^*}{\partial \xi_1^*}+\frac{U_2^*}{h_2}\frac{\partial U_2^*}{\partial \xi_2^*}+\frac{U_3^*}{h_3}\frac{\partial U_2^*}{\partial \xi_3^*}+U_2^*U_1^*\kappa_{21}^*+U_2^*U_3^*\kappa_{23}^*-U_1^*U_1^*\kappa_{12}^*-\varepsilon^2U_3^*U_3^*\kappa_{32}^* \\
&\quad=-\frac{1}{h_2}\frac{\partial p^*}{\partial \xi_2^*}+\frac{1}{Re}\left[\frac{1}{h}\frac{\partial}{\partial \xi_1^*}\left(\frac{h}{h_1}\tau_{21}^*\right)+\frac{1}{h}\frac{\partial}{\partial \xi_2^*}\left(\frac{h}{h_2}\tau_{22}^*\right)\right. \\
&\quad+\frac{1}{\varepsilon^2}\frac{1}{h}\frac{\partial}{\partial \xi_3^*}\left(\frac{h}{h_3}\frac{h_2}{h_3}\frac{\partial}{\partial \xi_3^*}\left(\frac{U_2^*}{h_2}\right)\right)+\frac{1}{h}\frac{\partial}{\partial \xi_3^*}\left(\frac{h}{h_3}\frac{h_3}{h_2}\frac{\partial}{\partial \xi_2^*}\left(\frac{U_3^*}{h_3}\right)\right) \\
&\quad\left.+\tau_{21}^*\kappa_{21}^*+\frac{1}{\varepsilon^2}\frac{h_2}{h_3}\frac{\partial}{\partial \xi_3^*}\left(\frac{U_2^*}{h_2}\right)\kappa_{23}^*+\frac{h_3}{h_2}\frac{\partial}{\partial \xi_2^*}\left(\frac{U_3^*}{h_3}\right)\kappa_{23}^*-\tau_{11}^*\kappa_{12}^*-\tau_{33}^*\kappa_{32}^*\right]
\end{aligned} \tag{4.7}$$

$$\begin{aligned}
&\varepsilon^2\frac{\partial U_3^*}{\partial t^*}+\varepsilon^2\frac{U_1^*}{h_1}\frac{\partial U_3^*}{\partial \xi_1^*}+\varepsilon^2\frac{U_2^*}{h_2}\frac{\partial U_3^*}{\partial \xi_2^*}+\varepsilon^2\frac{U_3^*}{h_3}\frac{\partial U_3^*}{\partial \xi_3^*}+\varepsilon^2U_3^*U_1^*\kappa_{31}^*+\varepsilon^2U_3^*U_2^*\kappa_{32}^*-U_1^*U_1^*\kappa_{13}^* \\
&\quad-U_2^*U_2^*\kappa_{23}^*=-\frac{1}{h_3}\frac{\partial p^*}{\partial \xi_3^*}+\frac{1}{Re}\left[\frac{1}{h}\frac{\partial}{\partial \xi_1^*}\left(\frac{h}{h_1}\frac{h_1}{h_3}\frac{\partial}{\partial \xi_3^*}\left(\frac{U_1^*}{h_1}\right)\right)\right. \\
&\quad+\varepsilon^2\frac{1}{h}\frac{\partial}{\partial \xi_1^*}\left(\frac{h}{h_1}\frac{h_3}{h_1}\frac{\partial}{\partial \xi_1^*}\left(\frac{U_3^*}{h_3}\right)\right)+\frac{1}{h}\frac{\partial}{\partial \xi_2^*}\left(\frac{h}{h_2}\frac{h_2}{h_3}\frac{\partial}{\partial \xi_3^*}\left(\frac{U_2^*}{h_2}\right)\right) \\
&\quad+\varepsilon^2\frac{1}{h}\frac{\partial}{\partial \xi_2^*}\left(\frac{h}{h_2}\frac{h_3}{h_2}\frac{\partial}{\partial \xi_2^*}\left(\frac{U_3^*}{h_3}\right)\right)+\frac{1}{h}\frac{\partial}{\partial \xi_3^*}\left(\frac{h}{h_3}\tau_{33}^*\right)+\frac{h_1}{h_3}\frac{\partial}{\partial \xi_3^*}\left(\frac{U_1^*}{h_1}\right)\kappa_{31}^* \\
&\quad+\varepsilon^2\frac{h_3}{h_1}\frac{\partial}{\partial \xi_1^*}\left(\frac{U_3^*}{h_3}\right)\kappa_{31}^*+\frac{h_2}{h_3}\frac{\partial}{\partial \xi_3^*}\left(\frac{U_2^*}{h_2}\right)\kappa_{32}^* \\
&\quad\left.+\varepsilon^2\frac{h_3}{h_2}\frac{\partial}{\partial \xi_2^*}\left(\frac{U_3^*}{h_3}\right)\kappa_{32}^*-\tau_{11}^*\kappa_{13}^*-\tau_{22}^*\kappa_{23}^*\right]
\end{aligned} \tag{4.8}$$

where $\varepsilon = ak$ is the wave slope and $Re = U_{10}/\nu k$ is the wave Reynolds number based on the wind speed at 10-m height. The wave Reynolds number is related to the wave roughness Reynolds numbers, first introduced by Zhao & Toba (2001), through,

$$Re = \frac{Re_H}{4C_d^{1/2}ak}$$

in which C_d is the air-sea drag coefficient and $Re_H = u_*H/\nu$ is the wave roughness Reynolds number where u_* is the friction velocity and $H = 4a$ is proportional to the significant wave height. A non-dimensionalized equation for the kinetic energy budget can be similarly derived. It is not presented here for the sake of brevity as it leads to a long and tedious derivation. Choosing a vertical length scale small compared to the horizontal length scale ($ak \ll 1$) implies that the range of validity of the boundary layer equations is limited to $k\xi_3 \approx \mathrm{O}(ak)$, i.e. approximately within a wave height of the surface. Wave-coherent motions are known to penetrate the airflow up to heights on the order of the wavelength rather than the wave height; the coordinate transformations, just like wave-induced motion, do indeed show an $\exp(-k\xi_3)$ dependency. Instead, the boundary layer scaling offered here is intended to be utilized to evaluate, for example, the scale of high order terms such as Reynolds and wave stresses compared to viscous stresses. In fact, although the viscous stress in the airflow over wind-generated waves has been the topic of many studies over the past decades (e.g., Longuet-Higgins 1969; Hsu & Hsu 1983; Banner 1990; Banner & Peirson 1998; Veron *et al.* 2007; Buckley & Veron 2016), it has just recently been shown that the contribution of the viscous stress to the total air-water momentum flux is not negligible, at least in low wind speeds (Grare *et al.* 2013; Buckley & Veron 2017). Therefore, in order to retain the

viscous effects in the boundary layer equations, the largest viscous term is required to be of the same order of magnitude as the inertia terms, i.e. $1/Re$ must be of the order of magnitude of ε^2.

In order to pursue the order of magnitude analysis, it is also necessary to determine the order of magnitude of scale factors and curvature parameters in equations (4.5) to (4.8) and the kinetic energy budget equation. To this end, the specifics of the coordinate transformation need to be prescribed.

Following Benjamin (1959), we adopt an orthogonal wave-following coordinate system in the frame of reference moving with the wave,

$$\begin{aligned}\xi_1 &= x_1 - iae^{i(k_1x_1+k_2x_2)}e^{-kx_3}\\ \xi_2 &= x_2 - iae^{i(k_1x_1+k_2x_2)}e^{-kx_3}\\ \xi_3 &= x_3 - ae^{i(k_1x_1+k_2x_2)}e^{-kx_3}\end{aligned} \tag{4.9}$$

where (ξ_1,ξ_2,ξ_3) are wave-following coordinates, (x_1,x_2,x_3) are rectangular coordinates, k_1 is the wavenumber in streamwise direction, k_2 is wavenumber in the lateral direction, and $k = |\boldsymbol{k}|$ is the wavenumber. The actual wave profile is, to the first order in ak, given by $\xi_3 = 0$. This type of coordinate transformation is thoroughly used in the literature (e.g., Belcher & Hunt 1993; Belcher *et al.* 1993; Sullivan *et al.* 2000; Tseluiko & Kalliadasis 2011; Náraigh *et al.* 2011) as it permits a linear analysis for small-slope waves. Considering $ak_1 \sim ak_2 \sim ak$ are of the same order, say ε, and retaining first-order terms, the coordinate differential can be expressed as,

$$\begin{bmatrix}\frac{\partial x_1}{\partial \xi_1} & \frac{\partial x_1}{\partial \xi_2} & \frac{\partial x_1}{\partial \xi_3}\\ \frac{\partial x_2}{\partial \xi_1} & \frac{\partial x_2}{\partial \xi_2} & \frac{\partial x_2}{\partial \xi_3}\\ \frac{\partial x_3}{\partial \xi_1} & \frac{\partial x_3}{\partial \xi_2} & \frac{\partial x_3}{\partial \xi_3}\end{bmatrix} \approx \begin{bmatrix}1-\varepsilon e^{i\varphi}e^{-k\xi_3} & -\varepsilon e^{i\varphi}e^{-k\xi_3} & -i\varepsilon e^{i\varphi}e^{-k\xi_3}\\ -\varepsilon e^{i\varphi}e^{-k\xi_3} & 1-\varepsilon e^{i\varphi}e^{-k\xi_3} & -i\varepsilon e^{i\varphi}e^{-k\xi_3}\\ i\varepsilon e^{i\varphi}e^{-k\xi_3} & i\varepsilon e^{i\varphi}e^{-k\xi_3} & 1-\varepsilon e^{i\varphi}e^{-k\xi_3}\end{bmatrix} + \mathrm{O}(\varepsilon^2) \tag{4.10}$$

where $\varphi = (k_1\xi_1 + k_2\xi_2)$. Consequently, the scale factors, introduced in equations (2.6), are of the order of,

$$h_i \approx 1 + \mathrm{O}(\varepsilon) \tag{4.11}$$

The order of magnitude of dimensionless curvature parameters (2.13) can be further estimated,

$$\begin{aligned}\mathcal{K}^* &= \begin{bmatrix}\frac{1}{h_1}\frac{1}{h_1}\frac{\partial h_1}{\partial \xi_1^*} & \frac{1}{h_1}\frac{1}{h_2}\frac{\partial h_1}{\partial \xi_2^*} & \frac{1}{h_1}\frac{1}{h_3}\frac{\partial h_1}{\partial \xi_3^*}\\ \frac{1}{h_1}\frac{1}{h_2}\frac{\partial h_2}{\partial \xi_1^*} & \frac{1}{h_2}\frac{1}{h_2}\frac{\partial h_2}{\partial \xi_2^*} & \frac{1}{h_2}\frac{1}{h_3}\frac{\partial h_2}{\partial \xi_3^*}\\ \frac{1}{h_1}\frac{1}{h_3}\frac{\partial h_3}{\partial \xi_1^*} & \frac{1}{h_2}\frac{1}{h_3}\frac{\partial h_3}{\partial \xi_2^*} & \frac{1}{h_3}\frac{1}{h_3}\frac{\partial h_3}{\partial \xi_3^*}\end{bmatrix}\\ &\approx \begin{bmatrix}-2i\varepsilon e^{i\varphi^*}e^{-\varepsilon\xi_3^*} + \mathrm{O}(\varepsilon^2) & -2i\varepsilon e^{i\varphi^*}e^{-\varepsilon\xi_3^*} + \mathrm{O}(\varepsilon^2) & 2\varepsilon^2 e^{i\varphi^*}e^{-\varepsilon\xi_3^*} + \mathrm{O}(\varepsilon^3)\\ -2i\varepsilon e^{i\varphi^*}e^{-\varepsilon\xi_3^*} + \mathrm{O}(\varepsilon^2) & -2i\varepsilon e^{i\varphi^*}e^{-\varepsilon\xi_3^*} + \mathrm{O}(\varepsilon^2) & 2\varepsilon^2 e^{i\varphi^*}e^{-\varepsilon\xi_3^*} + \mathrm{O}(\varepsilon^3)\\ -2i\varepsilon e^{i\varphi^*}e^{-\varepsilon\xi_3^*} + \mathrm{O}(\varepsilon^2) & -2i\varepsilon e^{i\varphi^*}e^{-\varepsilon\xi_3^*} + \mathrm{O}(\varepsilon^2) & 2\varepsilon^2 e^{i\varphi^*}e^{-\varepsilon\xi_3^*} + \mathrm{O}(\varepsilon^3)\end{bmatrix}\end{aligned} \tag{4.12}$$

where $\varphi^* = (\xi_1^* + \xi_2^*)$. Thus $\kappa_{i3}^* \sim \mathrm{O}(\varepsilon^2)$ and all other dimensionless curvature parameters are of order $\mathrm{O}(\varepsilon)$. The order of magnitude analysis can now be thoroughly established for the terms

involving the scale factor and curvature parameter. The details of estimating the order of scale factors and their derivatives can be found in Tseluiko & Kalliadasis (2011) and Náraigh *et al.* (2011).

We note here that the transformation outlined above (equation 4.9) is valid for monochromatic waves. In the case of wind waves, however, multi-modal transformations are generally utilized. For example, this was done in the work of Sullivan *et al.* (2014, 2018) for numerical simulations and in the study by Buckley & Veron (2016) for experimental studies. Extending the transformation (4.9) to a summation of multiple Fourier modes of amplitude a_n and wavenumber k_n leads to $h_i \approx 1 + \mathrm{O}(\sum a_n k_n)$. Because of the specifics of the spectral shape for wind waves (i.e. $k^{-5/2}$ to k^{-3} above the wave peak in the equilibrium and saturation ranges), $h_i \approx 1 + \mathrm{O}(a_p k_p)$ where a_p and k_p are respectively the peak amplitude and wavenumber.

We are now in a position to complete an order of magnitude analysis for the governing equations. Neglecting all terms with the order of magnitude of $\mathrm{O}(\varepsilon^2)$ and higher yields the governing equations for the flow over wind-generated surface waves with modest slopes. Therefore, the governing equations in terms of dimensional variables are reduced to the following forms for continuity equation,

$$\frac{1}{h}\frac{\partial}{\partial \xi_1}\left(\frac{h}{h_1}U_1\right) + \frac{1}{h}\frac{\partial}{\partial \xi_2}\left(\frac{h}{h_2}U_2\right) + \frac{1}{h_3}\frac{\partial U_3}{\partial \xi_3} = 0 \tag{4.13}$$

momentum equations,

$$\begin{aligned}\frac{\partial U_1}{\partial t} + \frac{U_1}{h_1}\frac{\partial U_1}{\partial \xi_1} + \frac{U_2}{h_2}\frac{\partial U_1}{\partial \xi_2} + \frac{U_3}{h_3}\frac{\partial U_1}{\partial \xi_3} + (U_1 U_2 \kappa_{12} - U_2 U_2 \kappa_{21}) \\ = -\frac{1}{\rho}\frac{1}{h_1}\frac{\partial p}{\partial \xi_1} + \nu\frac{1}{h_3}\frac{1}{h_3}\frac{\partial}{\partial \xi_3}\left(\frac{\partial U_1}{\partial \xi_3}\right)\end{aligned} \tag{4.14}$$

$$\begin{aligned}\frac{\partial U_2}{\partial t} + \frac{U_1}{h_1}\frac{\partial U_2}{\partial \xi_1} + \frac{U_2}{h_2}\frac{\partial U_2}{\partial \xi_2} + \frac{U_3}{h_3}\frac{\partial U_2}{\partial \xi_3} + (U_2 U_1 \kappa_{21} - U_1 U_1 \kappa_{12}) \\ = -\frac{1}{\rho}\frac{1}{h_2}\frac{\partial p}{\partial \xi_2} + \nu\frac{1}{h_3}\frac{1}{h_3}\frac{\partial}{\partial \xi_3}\left(\frac{\partial U_2}{\partial \xi_3}\right)\end{aligned} \tag{4.15}$$

$$\frac{1}{\rho}\frac{1}{h_3}\frac{\partial p}{\partial \xi_3} = 0 \tag{4.16}$$

and kinetic energy equation,

$$\frac{\partial e}{\partial t} + \frac{U_i}{h_{(i)}}\frac{\partial e}{\partial \xi_i} = -\frac{1}{\rho}\frac{U_i}{h_{(i)}}\frac{\partial p}{\partial \xi_i} + \frac{\nu}{h_3 h_3}\left[U_1\frac{\partial}{\partial \xi_3}\left(\frac{\partial U_1}{\partial \xi_3}\right) + U_2\frac{\partial}{\partial \xi_3}\left(\frac{\partial U_2}{\partial \xi_3}\right)\right] \tag{4.17}$$

In which,

$$e = \frac{1}{2}U_1 U_1 + \frac{1}{2}U_2 U_2$$

is the kinetic energy. We note here that equations (4.14) through (4.17) reduce to the conventional boundary layer equations in the rectangular coordinates at order $\mathrm{O}(1)$. These equations can be compared with the viscous boundary-layer equations over a solid curved surface derived by, for example, Cebeci *et al.* (1976), Degani & Walker (1993), and Cebeci & Cousteix (2005).

4.1. *Triple decomposition*

The boundary layer equations above can also be decomposed into mean, wave-induced, and turbulent components by using the triple decomposition technique introduced in section 3. Before proceeding with the triple decomposition of continuity, momentum, and energy equations, however, we need to introduce a new set of dimensionless variables since employing the triple decomposition technique leads to the double correlation of wave and turbulent velocities including the turbulent and wave stresses. Experiments (e.g., Buckley & Veron 2017, 2019) indicate that, across the boundary layer, the mean velocity component in the vertical direction can be assumed to be smaller than the streamwise and lateral mean velocity components, while the wave-induced and turbulent velocities are presumably all of the same order of magnitude and much smaller than the horizontal mean velocities. The triple decomposed equations will be then non-dimensionalized, very much in the same manner as before, but using the following dimensionless variables,

$$\xi_1^* = k\xi_1, \qquad \xi_2^* = k\xi_2, \qquad \xi_3^* = \frac{\xi_3}{a} \tag{4.18}$$

$$\overline{U}_1^* = \frac{\overline{U}_1}{U_{10}}, \qquad \overline{U}_2^* = \frac{\overline{U}_2}{U_{10}}, \qquad \overline{U}_3^* = \frac{\overline{U}_3}{akU_{10}} \tag{4.19}$$

$$\widetilde{U}_1^* = \frac{\widetilde{U}_1}{akU_{10}}, \qquad \widetilde{U}_2^* = \frac{\widetilde{U}_2}{akU_{10}}, \qquad \widetilde{U}_3^* = \frac{\widetilde{U}_3}{akU_{10}} \tag{4.20}$$

$$U_1'^* = \frac{U_1'}{akU_{10}}, \qquad U_2'^* = \frac{U_2'}{akU_{10}}, \qquad U_3'^* = \frac{U_3'}{akU_{10}} \tag{4.21}$$

$$\bar{p}^* = \frac{\bar{p}}{\rho U_{10}^2}, \qquad \tilde{p}^* = \frac{\tilde{p}}{\rho U_{10}^2 ak}, \qquad p'^* = \frac{p'}{\rho U_{10}^2 ak} \tag{4.22}$$

$$t^* = U_{10}kt \tag{4.23}$$

The continuity equations for the mean, wave, and turbulent flow fields can be readily obtained by substituting the decomposed velocities into the continuity equation (4.13) and then applying the ensemble- and phase-average operators,

$$\frac{1}{h}\frac{\partial}{\partial\xi_1}\left(\frac{h}{h_1}\overline{U}_1\right) + \frac{1}{h}\frac{\partial}{\partial\xi_2}\left(\frac{h}{h_2}\overline{U}_2\right) + \frac{1}{h_3}\frac{\partial\overline{U}_3}{\partial\xi_3} = 0 \tag{4.24}$$

$$\frac{1}{h}\frac{\partial}{\partial\xi_1}\left(\frac{h}{h_1}\widetilde{U}_1\right) + \frac{1}{h}\frac{\partial}{\partial\xi_2}\left(\frac{h}{h_2}\widetilde{U}_2\right) + \frac{1}{h_3}\frac{\partial\widetilde{U}_3}{\partial\xi_3} = 0 \tag{4.25}$$

$$\frac{1}{h}\frac{\partial}{\partial\xi_1}\left(\frac{h}{h_1}U_1'\right) + \frac{1}{h}\frac{\partial}{\partial\xi_2}\left(\frac{h}{h_2}U_2'\right) + \frac{1}{h_3}\frac{\partial U_3'}{\partial\xi_3} = 0 \tag{4.26}$$

Deriving the decomposed momentum and energy budget equations for the boundary layer, however, requires more effort. Following substituting the decomposed fields into the momentum equations (4.14) and (4.15) and applying the ensemble and phase averaging operators, it is necessary to perform the order of magnitude analysis using the dimensionless variables introduced in equations (4.18) to (4.23) due to the new double-velocity correlation expressions. The details, however, is eliminated to keep the brevity. Neglecting all terms with the order of magnitude of $\mathrm{O}\left(\varepsilon^2\right)$ and higher renders the ξ_3 equations trivial. The mean momentum equations in ξ_1 and ξ_2 directions can be expressed as,

$$\frac{\partial \overline{U}_1}{\partial t}+\frac{\overline{U}_j}{h_{(j)}}\frac{\partial \overline{U}_1}{\partial \xi_j}+\left(\overline{U}_1\overline{U}_2\kappa_{12}-\overline{U}_2\overline{U}_2\kappa_{21}\right)+\frac{1}{h_3}\frac{\partial}{\partial \xi_3}\left(\overline{\tilde{U}_1\tilde{U}_3}\right)+\frac{1}{h_3}\frac{\partial}{\partial \xi_3}\left(\overline{U_1'U_3'}\right)$$
$$=-\frac{1}{\rho}\frac{1}{h_1}\frac{\partial \overline{p}}{\partial \xi_1}+\nu\frac{1}{h_3}\frac{1}{h_3}\frac{\partial}{\partial \xi_3}\left(\frac{\partial \overline{U}_1}{\partial \xi_3}\right) \tag{4.27}$$

$$\frac{\partial \overline{U}_2}{\partial t}+\frac{\overline{U}_j}{h_{(j)}}\frac{\partial \overline{U}_2}{\partial \xi_j}+\left(\overline{U}_2\overline{U}_1\kappa_{21}-\overline{U}_1\overline{U}_1\kappa_{12}\right)+\frac{1}{h_3}\frac{\partial}{\partial \xi_3}\left(\overline{\tilde{U}_2\tilde{U}_3}\right)+\frac{1}{h_3}\frac{\partial}{\partial \xi_3}\left(\overline{U_2'U_3'}\right)$$
$$=-\frac{1}{\rho}\frac{1}{h_2}\frac{\partial \overline{p}}{\partial \xi_2}+\nu\frac{1}{h_3}\frac{1}{h_3}\frac{\partial}{\partial \xi_3}\left(\frac{\partial \overline{U}_2}{\partial \xi_3}\right) \tag{4.28}$$

Applying the phase-averaged operator to the decomposed wave-induced momentum equations (4.14) and (4.15), subtracting the mean momentum equations, and neglecting terms of order $\mathrm{O}\left(\varepsilon^2\right)$, the wave momentum equations can be written as,

$$\frac{\partial \widetilde{U}_1}{\partial t}+\frac{\widetilde{U}_j}{h_{(j)}}\frac{\partial \overline{U}_1}{\partial \xi_j}+\left(\overline{U}_1\widetilde{U}_2\kappa_{12}-\overline{U}_2\widetilde{U}_2\kappa_{21}\right)+\frac{\overline{U}_j}{h_{(j)}}\frac{\partial \widetilde{U}_1}{\partial \xi_j}+\left(\widetilde{U}_1\overline{U}_2\kappa_{12}-\widetilde{U}_2\overline{U}_2\kappa_{21}\right)$$
$$+\frac{1}{h_3}\frac{\partial \tilde{R}_{13}}{\partial \xi_3}+\frac{1}{h_3}\frac{\partial \tilde{r}_{13}}{\partial \xi_3}=-\frac{1}{\rho}\frac{1}{h_1}\frac{\partial \tilde{p}}{\partial \xi_1}+\nu\frac{1}{h_3}\frac{1}{h_3}\frac{\partial}{\partial \xi_3}\left(\frac{\partial \widetilde{U}_1}{\partial \xi_3}\right) \tag{4.29}$$

$$\frac{\partial \widetilde{U}_2}{\partial t}+\frac{\widetilde{U}_j}{h_{(j)}}\frac{\partial \overline{U}_2}{\partial \xi_j}+\left(\overline{U}_2\widetilde{U}_1\kappa_{21}-\overline{U}_1\widetilde{U}_1\kappa_{12}\right)+\frac{\overline{U}_j}{h_{(j)}}\frac{\partial \widetilde{U}_2}{\partial \xi_j}+\left(\widetilde{U}_2\overline{U}_1\kappa_{21}-\widetilde{U}_1\overline{U}_1\kappa_{12}\right)$$
$$+\frac{1}{h_3}\frac{\partial \tilde{R}_{23}}{\partial \xi_3}+\frac{1}{h_3}\frac{\partial \tilde{r}_{23}}{\partial \xi_3}=-\frac{1}{\rho}\frac{1}{h_2}\frac{\partial \tilde{p}}{\partial \xi_2}+\nu\frac{1}{h_3}\frac{1}{h_3}\frac{\partial}{\partial \xi_3}\left(\frac{\partial \widetilde{U}_2}{\partial \xi_3}\right) \tag{4.30}$$

In these equations $\tilde{r}_{ij}=\langle U_i'U_j'\rangle-\overline{U_i'U_j'}$ and $\tilde{R}_{ij}=\langle \widetilde{U}_i\widetilde{U}_j\rangle-\overline{\tilde{U}_i\tilde{U}_j}$. Finally, we are deriving the momentum equation for the background turbulence in the boundary layer by subtracting the mean and wave momentum equations from the decomposed momentum equations and neglecting terms of order $\mathrm{O}\left(\varepsilon^2\right)$. Consequently, the momentum equations for the turbulent field can be written in ξ_1 and ξ_2 directions as,

$$\frac{\partial U_1'}{\partial t}+\frac{U_j'}{h_{(j)}}\frac{\partial \overline{U}_1}{\partial \xi_j}+\left(\overline{U}_1U_2'\kappa_{12}-\overline{U}_2U_2'\kappa_{21}\right)+\frac{\overline{U}_j}{h_{(j)}}\frac{\partial U_1'}{\partial \xi_j}+\left(U_1'\overline{U}_2\kappa_{12}-U_2'\overline{U}_2\kappa_{21}\right)$$
$$+\frac{1}{h_3}\frac{\partial}{\partial \xi_3}\left(\widetilde{U}_1U_3'\right)+\frac{1}{h_3}\frac{\partial}{\partial \xi_3}\left(U_1'\widetilde{U}_3\right)+\frac{1}{h_3}\frac{\partial}{\partial \xi_3}\left(U_1'U_3'\right)$$
$$-\frac{1}{h_3}\frac{\partial}{\partial \xi_3}\left(\langle U_1'U_3'\rangle\right)=-\frac{1}{\rho}\frac{1}{h_1}\frac{\partial p'}{\partial \xi_1}+\nu\frac{1}{h_3}\frac{1}{h_3}\frac{\partial}{\partial \xi_3}\left(\frac{\partial U_1'}{\partial \xi_3}\right) \tag{4.31}$$

$$\begin{aligned}\frac{\partial U_2'}{\partial t}+\frac{U_j'}{h_{(j)}}\frac{\partial \overline{U}_2}{\partial \xi_j}+\left(\overline{U}_2U_1'\kappa_{21}-\overline{U}_1U_1'\kappa_{12}\right)+\frac{\overline{U}_j}{h_{(j)}}\frac{\partial U_2'}{\partial \xi_j}+\left(U_2'\overline{U}_1\kappa_{21}-U_1'\overline{U}_1\kappa_{12}\right)\\ +\frac{1}{h_3}\frac{\partial}{\partial \xi_3}\left(\widetilde{U}_2U_3'\right)+\frac{1}{h_3}\frac{\partial}{\partial \xi_3}\left(U_2'\widetilde{U}_3\right)+\frac{1}{h_3}\frac{\partial}{\partial \xi_3}\left(U_2'U_3'\right)\\ -\frac{1}{h_3}\frac{\partial}{\partial \xi_3}\left(\langle U_2'U_3'\rangle\right)=-\frac{1}{\rho}\frac{1}{h_2}\frac{\partial p'}{\partial \xi_2}+\nu\frac{1}{h_3}\frac{1}{h_3}\frac{\partial}{\partial \xi_3}\left(\frac{\partial U_2'}{\partial \xi_3}\right)\end{aligned}\tag{4.32}$$

In addition, the mean viscous stress, which appears in equation (4.27), can be shown to reduce to,

$$\tau_{13}=\nu\frac{1}{h_3}\frac{\partial \overline{U}_1}{\partial \xi_3}\approx\nu\frac{\partial \overline{U}_1}{\partial \xi_3}\left(1+\mathrm{O}(\varepsilon)\right)+\mathrm{O}(\varepsilon^2)$$

which to the leading order is,

$$\tau_{13}\approx\nu\frac{\partial \overline{U}_1}{\partial \xi_3}\tag{4.33}$$

An equation for the mean, wave, and turbulent kinetic energy budgets for the flow in the boundary layer can be also obtained by multiplying the mean, wave, and turbulent momentum equations by the mean, wave-induced and turbulent velocities, respectively, and then successively applying the phase- and ensemble-averaging operators,

$$\begin{aligned}\frac{\partial \bar{e}}{\partial t}+\frac{\overline{U}_j}{h_{(j)}}\frac{\partial \bar{e}}{\partial \xi_j}+\frac{\overline{U}_1}{h_3}\frac{\partial \overline{T}_{13}}{\partial \xi_3}+\frac{\overline{U}_2}{h_3}\frac{\partial \overline{T}_{23}}{\partial \xi_3}\\ =-\frac{1}{\rho}\frac{\overline{U}_j}{h_{(j)}}\frac{\partial \overline{p}}{\partial \xi_j}+\frac{\nu}{h_3h_3}\left[\overline{U}_1\frac{\partial}{\partial \xi_3}\left(\frac{\partial \overline{U}_1}{\partial \xi_3}\right)+\overline{U}_2\frac{\partial}{\partial \xi_3}\left(\frac{\partial \overline{U}_2}{\partial \xi_3}\right)\right]\end{aligned}\tag{4.34}$$

$$\begin{aligned}\frac{D\tilde{\bar{e}}}{Dt}+\frac{\overline{\tilde{U}_j\tilde{U}_1}}{h_{(j)}}\frac{\partial \overline{U}_1}{\partial \xi_j}+\left(\overline{\tilde{U}_2\tilde{U}_2}\overline{U}_1\kappa_{21}-\overline{\tilde{U}_2\tilde{U}_1}\overline{U}_1\kappa_{12}\right)+\frac{\overline{\tilde{U}_j\tilde{U}_2}}{h_{(j)}}\frac{\partial \overline{U}_2}{\partial \xi_j}\\ +\left(\overline{\tilde{U}_1\tilde{U}_1}\overline{U}_2\kappa_{12}-\overline{\tilde{U}_1\tilde{U}_2}\overline{U}_2\kappa_{21}\right)+\overline{\frac{\tilde{U}_1}{h_3}\frac{\partial \tilde{T}_{13}}{\partial \xi_3}}+\overline{\frac{\tilde{U}_2}{h_3}\frac{\partial \tilde{T}_{23}}{\partial \xi_3}}\\ =-\frac{1}{\rho}\overline{\frac{\tilde{U}_j}{h_{(j)}}\frac{\partial \tilde{p}}{\partial \xi_j}}+\frac{\nu}{h_3h_3}\left[\overline{\tilde{U}_1\frac{\partial}{\partial \xi_3}\left(\frac{\partial \tilde{U}_1}{\partial \xi_3}\right)}+\overline{\tilde{U}_2\frac{\partial}{\partial \xi_3}\left(\frac{\partial \tilde{U}_2}{\partial \xi_3}\right)}\right]\end{aligned}\tag{4.35}$$

$$\begin{aligned}
&\frac{D\overline{e'}}{Dt}+\frac{\overline{U_j'U_1'}}{h_{(j)}}\frac{\partial\overline{U}_1}{\partial\xi_j}+\left(\overline{U_2'U_2'}\overline{U}_1\kappa_{21}-\overline{U_2'U_1'}\overline{U}_1\kappa_{12}\right)+\frac{\overline{U_j'U_2'}}{h_{(j)}}\frac{\partial\overline{U}_2}{\partial\xi_j}\\
&\quad+\left(\overline{U_1'U_1'}\overline{U}_2\kappa_{12}-\overline{U_1'U_2'}\overline{U}_2\kappa_{21}\right)+\overline{\frac{U_1'}{h_3}\frac{\partial}{\partial\xi_3}\left(\tilde{U}_1U_3'\right)}\\
&\quad+\overline{\frac{U_1'}{h_3}\frac{\partial}{\partial\xi_3}\left(U_1'\tilde{U}_3\right)}+\overline{\frac{U_1'}{h_3}\frac{\partial}{\partial\xi_3}\left(U_1'U_3'\right)}+\overline{\frac{U_2'}{h_3}\frac{\partial}{\partial\xi_3}\left(\tilde{U}_2U_3'\right)}\\
&\quad+\overline{\frac{U_2'}{h_3}\frac{\partial}{\partial\xi_3}\left(U_2'\tilde{U}_3\right)}+\overline{\frac{U_2'}{h_3}\frac{\partial}{\partial\xi_3}\left(U_2'U_3'\right)}\\
&\quad=-\frac{1}{\rho}\overline{\frac{U_j'}{h_{(j)}}\frac{\partial p'}{\partial\xi_j}}+\frac{\nu}{h_3h_3}\left[\overline{U_1'\frac{\partial}{\partial\xi_3}\left(\frac{\partial U_1'}{\partial\xi_3}\right)}+\overline{U_2'\frac{\partial}{\partial\xi_3}\left(\frac{\partial U_2'}{\partial\xi_3}\right)}\right]
\end{aligned}\tag{4.36}$$

where,

$$T_{ij}=\widetilde{U}_i\widetilde{U}_j+U_i'U_j'$$

is the total fluctuation stress tensor, and,

$$\bar{e}=\frac{1}{2}\overline{U}_1\overline{U}_1+\frac{1}{2}\overline{U}_2\overline{U}_2$$

$$\tilde{e}=\frac{1}{2}\widetilde{U}_1\widetilde{U}_1+\frac{1}{2}\widetilde{U}_2\widetilde{U}_2+\frac{1}{2}\widetilde{U}_3\widetilde{U}_3$$

$$e'=\frac{1}{2}U_1'U_1'+\frac{1}{2}U_2'U_2'+\frac{1}{2}U_3'U_3'$$

are the mean, wave-induced, and turbulent kinetic energy, respectively. Moreover, D/Dt is the mean material derivative defined in equation (3.8). The readers should note that deriving the triple-decomposed equations, particularly energy budget equations, in an orthogonal curvilinear coordinate system describing the fluid motion in the boundary layer is an exercise that, while straightforward, is quite tedious. The details of the derivation are omitted here for the sake of brevity but are available upon request.

4.2. *Validation of scale analysis*

The equations for the mean, wave-induced, and turbulent flows in the boundary layer adjacent to surface waves with modest slopes (equations 4.27 to 4.32) were derived by assuming that terms $\mathrm{O}\left(\varepsilon^2\right)$ and higher are negligible. In this section, we assess some of these assumptions using the experimental laboratory data of Buckley & Veron (2016, 2017) who have measured two-dimensional velocity fields in the airflow above moving surface waves for different wind-wave conditions with wind speeds ranging from $\mathrm{U}_{10}=0.89$ m s^{-1} to $\mathrm{U}_{10}=16.59$ m s^{-1}. To this end, the measured velocity fields were projected and transformed into the curvilinear coordinate system, then averaged in the ξ-direction. A detailed analysis of these experimental data is presented in the companion paper (Yousefi *et al.* 2019). For the mean momentum equation in ξ_1-direction (equation 4.27), for example, the complete dimensionless equation (in 2D) is,

$$\frac{\partial \overline{U}_1^*}{\partial t^*}+\frac{1}{h}\frac{\partial}{\partial \xi_1^*}\left(\frac{h}{h_1}\overline{U}_1^*\overline{U}_1^*\right)+\frac{1}{h}\frac{\partial}{\partial \xi_3^*}\left(\frac{h}{h_3}\overline{U}_1^*\overline{U}_3^*\right)+\left(\overline{U}_1^*\overline{U}_3^*\kappa_{13}^*-\varepsilon^2\overline{U}_3^*\overline{U}_3^*\kappa_{31}^*\right)$$
$$+\varepsilon^2\underbrace{\frac{1}{h}\frac{\partial}{\partial \xi_1^*}\left(\frac{h}{h_1}\overline{\tilde{U}_1^*\tilde{U}_1^*}\right)}_{\mathbf{I}}+\varepsilon\underbrace{\frac{1}{h}\frac{\partial}{\partial \xi_3^*}\left(\frac{h}{h_3}\overline{\tilde{U}_1^*\tilde{U}_3^*}\right)}_{\mathbf{II}}+\underbrace{\left(\varepsilon\overline{\tilde{U}_1^*\tilde{U}_3^*}\kappa_{13}^*-\varepsilon^2\overline{\tilde{U}_3^*\tilde{U}_3^*}\kappa_{31}^*\right)}_{\mathbf{III}}$$
$$+\varepsilon^2\underbrace{\frac{1}{h}\frac{\partial}{\partial \xi_1^*}\left(\frac{h}{h_1}\overline{U_1'^*U_1'^*}\right)}_{\mathbf{IV}}+\varepsilon^2\frac{1}{h}\frac{\partial}{\partial \xi_2^*}\left(\frac{h}{h_2}\overline{U_1'^*U_2'^*}\right)+\varepsilon\underbrace{\frac{1}{h}\frac{\partial}{\partial \xi_3^*}\left(\frac{h}{h_3}\overline{U_1'^*U_3'^*}\right)}_{\mathbf{V}}$$
$$+\varepsilon^2\left(\overline{U_1'^*U_1'^*}\kappa_{12}^*-\overline{U_2'^*U_2'^*}\kappa_{21}^*\right)+\underbrace{\left(\varepsilon\overline{U_1'^*U_3'^*}\kappa_{13}^*-\varepsilon^2\overline{U_3'^*U_3'^*}\kappa_{31}^*\right)}_{\mathbf{VI}}=-\frac{1}{h_1}\frac{\partial \bar{p}^*}{\partial \xi_1^*} \tag{4.37}$$
$$+\frac{1}{Re}\left[\frac{1}{h}\frac{\partial}{\partial \xi_1^*}\left(\frac{h}{h_1}\overline{\tau}_{11}^*\right)+\frac{1}{\varepsilon^2}\underbrace{\frac{1}{h}\frac{\partial}{\partial \xi_3^*}\left(\frac{h}{h_3}\frac{h_1}{h_3}\frac{\partial}{\partial \xi_3^*}\left(\frac{\overline{U}_1^*}{h_1}\right)\right)}_{\mathbf{T1}}\right.$$
$$\left.+\underbrace{\frac{1}{h}\frac{\partial}{\partial \xi_3^*}\left(\frac{h}{h_3}\frac{h_3}{h_1}\frac{\partial}{\partial \xi_1^*}\left(\frac{\overline{U}_3^*}{h_3}\right)\right)}_{\mathbf{T2}}+\frac{1}{\varepsilon^2}\underbrace{\frac{h_1}{h_3}\frac{\partial}{\partial \xi_3^*}\left(\frac{\overline{U}_1^*}{h_1}\right)\kappa_{13}^*}_{\mathbf{T3}}+\frac{h_3}{h_1}\frac{\partial}{\partial \xi_1^*}\left(\frac{\overline{U}_3^*}{h_3}\right)\kappa_{13}^*-\overline{\tau}_{33}^*\kappa_{31}^*\right]$$

in which,

$$\mathrm{T1}=\frac{1}{h}\frac{\partial}{\partial \xi_3^*}\left(\frac{h}{h_3}\frac{h_1}{h_3}\frac{\partial}{\partial \xi_3^*}\left(\frac{\overline{U}_1^*}{h_1}\right)\right)=\frac{1}{h_3}\frac{1}{h_3}\frac{\partial}{\partial \xi_3^*}\left(\frac{\partial \overline{U}_1^*}{\partial \xi_3^*}\right)+\frac{1}{h_3}\frac{\partial \overline{U}_1^*}{\partial \xi_3^*}\frac{1}{h_1h_3}\frac{\partial h_1}{\partial \xi_3^*}$$
$$+\frac{1}{h_3}\frac{\partial \overline{U}_1^*}{\partial \xi_3^*}\frac{1}{h_2h_3}\frac{\partial h_2}{\partial \xi_3^*}-\frac{1}{h_3}\frac{\partial \overline{U}_1^*}{\partial \xi_3^*}\frac{1}{h_3h_3}\frac{\partial h_3}{\partial \xi_3^*}-\frac{\overline{U}_1^*}{h_1}\frac{1}{h_3h_3}\frac{\partial}{\partial \xi_3^*}\left(\frac{\partial h_1}{\partial \xi_3^*}\right) \tag{4.38}$$
$$-\frac{1}{h_1h_3}\frac{\partial h_1}{\partial \xi_3^*}\frac{1}{h_3}\frac{\partial \overline{U}_1^*}{\partial \xi_3^*}-\frac{\overline{U}_1^*}{h_1h_3}\frac{\partial h_1}{\partial \xi_3^*}\frac{1}{h_2h_3}\frac{\partial h_2}{\partial \xi_3^*}+\frac{\overline{U}_1^*}{h_1h_3}\frac{\partial h_1}{\partial \xi_3^*}\frac{1}{h_3h_3}\frac{\partial h_3}{\partial \xi_3^*}$$

$$\mathrm{T2}=\frac{1}{h}\frac{\partial}{\partial \xi_3^*}\left(\frac{h}{h_3}\frac{h_3}{h_1}\frac{\partial}{\partial \xi_1^*}\left(\frac{\overline{U}_3^*}{h_3}\right)\right)$$
$$=\frac{1}{h_1h_3}\frac{\partial}{\partial \xi_3^*}\left(\frac{\partial \overline{U}_3^*}{\partial \xi_1^*}\right)+\frac{1}{h_1}\frac{\partial \overline{U}_3^*}{\partial \xi_1^*}\frac{1}{h_2h_3}\frac{\partial h_2}{\partial \xi_3^*}-\frac{\overline{U}_3^*}{h_3}\frac{1}{h_3h_1}\frac{\partial}{\partial \xi_3^*}\left(\frac{\partial h_3}{\partial \xi_1^*}\right) \tag{4.39}$$
$$-\frac{1}{h_3}\frac{\partial \overline{U}_3^*}{\partial \xi_3^*}\frac{1}{h_1h_3}\frac{\partial h_3}{\partial \xi_1^*}-\frac{\overline{U}_3^*}{h_2h_3}\frac{\partial h_2}{\partial \xi_3^*}\frac{1}{h_1h_3}\frac{\partial h_3}{\partial \xi_1^*}+\frac{\overline{U}_3^*}{h_3h_3}\frac{\partial h_3}{\partial \xi_3^*}\frac{1}{h_1h_3}\frac{\partial h_3}{\partial \xi_1^*}$$

$$\mathrm{T3}=\frac{h_1}{h_3}\frac{\partial}{\partial \xi_3^*}\left(\frac{\overline{U}_1^*}{h_1}\right)\kappa_{13}^*=\frac{1}{h_3}\frac{\partial \overline{U}_1^*}{\partial \xi_3^*}\kappa_{13}^*-\frac{\overline{U}_1^*}{h_1h_3}\frac{\partial h_1}{\partial \xi_3^*}\kappa_{13}^* \tag{4.40}$$

It is found from equation (4.37) that, for example, the derivative of the wave-induced stress with respect to the vertical direction (term II in equation 4.37) is an order of magnitude larger than the derivative of the horizontal wave-induced variance in the streamwise direction (term I in equation

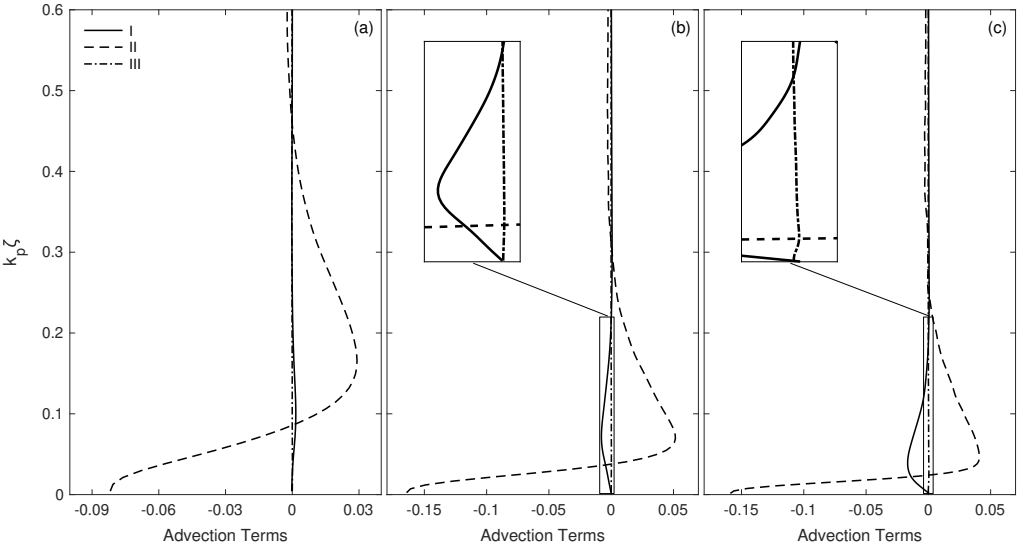

FIGURE 3. Vertical profiles of the streamwise divergence of horizontal wave-induced variance (term I), vertical divergence of wave-induced stress (term II), and additional wave-induced stresses (term III) for experiments with a wind speed of (a) $U_{10} = 2.25$ m s^{-1}, (b) $U_{10} = 5.08$ m s^{-1}, and (c) $U_{10} = 9.57$ m s^{-1} corresponding to a wave slope of (a) $\varepsilon = 0.07$, (b) $\varepsilon = 0.13$, and (c) $\varepsilon = 0.19$, respectively. Terms I, II, and III are defined as $h^{-1}\partial\left(h_3\tilde{U}_1^*\tilde{U}_1^*\right)/\partial\xi_1^*$, $h^{-1}\partial\left(h_1\overline{\tilde{U}_1^*\tilde{U}_3^*}\right)/\partial\xi_3^*$, and $\overline{\tilde{U}_1^*\tilde{U}_3^*}\kappa_{13}^* - \overline{\tilde{U}_3^*\tilde{U}_3^*}\kappa_{31}^*$, respectively. The additional wave-induced stresses term is appeared in the mean momentum equation due to the streamline curvature, which is asymptotically zero and hence negligible for the flow over surface waves with a small slope.

4.37). That means the streamwise divergence of the horizontal wave-induced variance and the vertical divergence of the wave-induced stress are, respectively,

$$\mathrm{I} = \frac{1}{h}\frac{\partial}{\partial\xi_1^*}\left(\frac{h}{h_1}\overline{\tilde{U}_1^*\tilde{U}_1^*}\right) \approx O\left(\varepsilon^2\right) \tag{4.41}$$

$$\mathrm{II} = \frac{1}{h}\frac{\partial}{\partial\xi_3^*}\left(\frac{h}{h_3}\overline{\tilde{U}_1^*\tilde{U}_3^*}\right) \approx O\left(\varepsilon\right) \tag{4.42}$$

while the additional wave stresses which appeared in the mean momentum equation due to the streamline curvature (term III in equation 4.37) are of the order of,

$$\mathrm{III} = \overline{\tilde{U}_1^*\tilde{U}_3^*}\kappa_{13}^* - \overline{\tilde{U}_3^*\tilde{U}_3^*}\kappa_{31}^* \approx O\left(\varepsilon^3\right) \tag{4.43}$$

where κ_{13}^* and κ_{31}^* are dimensionless curvature parameters. The terms represented in equations (4.41) to (4.43) are shown in figure 3 for experiments with the wind speed of $U_{10} = 2.25$ m s^{-1}, 5.08 m s^{-1}, and 9.57 m s^{-1} corresponding to a wave slope of 0.07, 0.13, and 0.19, respectively. From this figure, it can be observed that, of these three terms, the derivative of the wave stress by ξ_3 (II) exerts a significant influence on the momentum flux compared to the other terms. This is consistent with the analysis above. The absolute extremum of the wave stress derivative in the vertical direction happens very close to the surface and increases with the wave slope from 0.082 for $\varepsilon = 0.07$ to 0.159 for $\varepsilon = 0.19$. We also note that, consistent with the range of validity of the boundary layer equations, the scaling between terms I, II, and III, holds near the surface where $k_p\zeta \ll 1$.

In order to provide a detailed comparison of the order of magnitude of the streamwise divergence

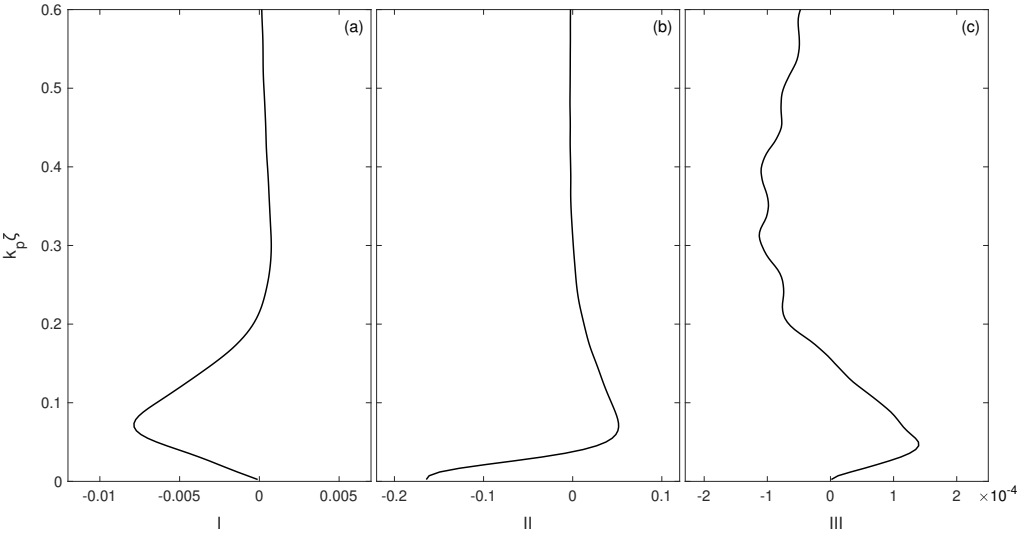

FIGURE 4. Vertical profiles of the (a) streamwise divergence of horizontal wave-induced variance (term I), (b) vertical divergence of wave-induced stress (term II), and (c) additional wave-induced stresses (term III) for the experiment with a wind speed of $U_{10} = 5.08$ m s^{-1} corresponding to a wave slope of $\varepsilon = 0.13$. Terms I, II, and III are defined as $h^{-1}\partial\left(h_3\overline{\tilde{U}_1^*\tilde{U}_1^*}\right)/\partial\xi_1^*$, $h^{-1}\partial\left(h_1\overline{\tilde{U}_1^*\tilde{U}_3^*}\right)/\partial\xi_3^*$, and $\overline{\tilde{U}_1^*\tilde{U}_3^*}\kappa_{13}^* - \overline{\tilde{U}_3^*\tilde{U}_3^*}\kappa_{31}^*$, respectively.

of horizontal wave-induced variance (term I), vertical divergence of wave-induced stress (term II), and additional wave-induced stresses (term III), the vertical profiles of these terms are further presented in figure 4 for the wind-wave condition of $U_{10} = 5.08$ m s^{-1} corresponding to a wave slope of $\varepsilon = 0.13$. In this experiment, term I is of the order of 0.008 ($\sim \varepsilon^2$), term II is of the order of 0.16 ($\sim \varepsilon$), and term III is of the order of 0.0014 ($\sim \varepsilon^3$). The terms with orders of magnitude larger than ε may not be fully resolved, in particular, for higher wind speeds due to the filtering processes in which a greater number of velocity fields contaminated by spray and other light reflections from the surface and thus excluded from the averaging process. The streamwise derivative of the horizontal wave-induced variance, and especially, the additional wave-induced stresses are almost zero everywhere except near the surface where the curvature effects are strong. They fall to zero from their maxima at a distance of nearly $k_p\zeta = 0.075$ and $k_p\zeta = 0.05$ for the term I and the term III, respectively.

Similarly, the streamwise divergence of the horizontal turbulent variance (term IV in equation 4.37), the vertical divergence of the turbulent stress (term V in equation 4.37), and the additional turbulent stresses (term VI in equation 4.37) are, respectively, of (leading) order of,

$$\mathrm{IV} = \frac{1}{h}\frac{\partial}{\partial\xi_1^*}\left(\frac{h}{h_1}\overline{U_1'^*U_1'^*}\right) \approx O\left(\varepsilon^2\right) \tag{4.44}$$

$$\mathrm{V} = \frac{1}{h}\frac{\partial}{\partial\xi_3^*}\left(\frac{h}{h_3}\overline{U_1'^*U_3'^*}\right) \approx O\left(\varepsilon\right) \tag{4.45}$$

$$\mathrm{VI} = \overline{U_1'^*U_3'^*}\kappa_{13}^* - \overline{U_3'^*U_3'^*}\kappa_{31}^* \approx O\left(\varepsilon^3\right) \tag{4.46}$$

The laboratory measurements of these terms are also consistent with the order of magnitude analysis; the divergence of the horizontal turbulent variance in the streamwise direction and the additional turbulent stresses are respectively one and two orders of magnitude smaller compared to the vertical divergence of the turbulent stress (not shown here to maintain brevity). Evidently,

the wave and turbulent stresses that appear because of curvature in the coordinate system, are asymptotically zero and hence negligible for the flow over surface waves with a small slope.

5. Conclusions

In the current work, the dynamical governing equations of three-dimensional fluid motion, i.e. the continuity, momentum, and kinetic energy equations, have been transformed into the orthogonal curvilinear coordinate system in such a way that flow direction and coordinate directions coincide. These equations are then separated into the mean, wave-induced, and turbulent components by employing the triple decomposition technique. The complete transformation of governing equations involves curvature parameters, or equivalently, the local radius of curvature and their higher order derivatives. The transformed equations therefore involve explicit extra geometric terms, for example, the additional production, advection, and diffusion terms representing the effects of streamline curvature on the structure of fluid flow including the acceleration of the mean flow. These formulations are valid down to the surface and naturally incorporate the curvature effects. Furthermore, the precise expressions for the mean, wave-induced, and turbulent viscous tresses are explicitly spelled out.

We also simplified considerably the continuity, momentum, and kinetic energy equations for the boundary-layer type flows based on the assumption that the vertical length scale of the motion is small compared to the horizontal length scale. Considering the flow over periodic surface waves wherein the wavelength of the disturbance is large compared to the wave amplitude, the order of magnitude analysis is then performed to derive the boundary layer equations in the orthogonal wave-following curvilinear coordinates. The boundary layer equations are also decomposed into the mean, wave-induced, and turbulent components. Implementing this triple decomposition leads to the appearance of double velocity correlations of wave and turbulent velocities that requires to be treated with the assumption that wave-induced and turbulent velocity components are all of the same order.

This research was supported by the National Science Foundation (NSF) through grant numbers of OCE-1458977 and OCE-1634051.

Appendix A.

The momentum equation in orthogonal curvilinear coordinates, described in equation (2.15), can be alternatively represented in terms of velocity and vorticity for an incompressible fluid using the compact notation introduced in section 2. The formulation of the Navier-Stokes equations in terms of velocity and vorticity is an interesting alternative form for numerical studies (e.g., Nikitin *et al.* 2009; Nikitin 2011). Using the summation notation introduced in section 2.1, the momentum equation in an orthogonal curvilinear coordinate system can be expressed in velocity-vorticity formulation as,

$$\frac{\partial U_i}{\partial t} + \frac{h_{(i)}h_{(j)}}{h} 2\Omega_{ij}U_j = -\frac{1}{\rho}\frac{1}{h_{(i)}}\frac{\partial p}{\partial \xi_i} - \boldsymbol{\nabla}\left(\frac{1}{2}|\boldsymbol{u}|^2\right) + 2\nu\frac{h_{(i)}}{h}\frac{\partial \Omega_{ij}}{\partial \xi_j} \tag{A 1}$$

where the components of the vorticity tensor $\boldsymbol{\Omega}$ can be expressed by,

$$\Omega_{ij} = -\frac{1}{2}\varepsilon_{ijk}h_{(k)}\omega_k \tag{A 2}$$

in which ε_{ijk} is the Levi-Civita permutation symbol. In order to complete the velocity-vorticity formulations, we further express the vorticity transport equation as,

$$\frac{\partial \omega_i}{\partial t} + \frac{U_j}{h_{(j)}} \frac{\partial \omega_i}{\partial \xi_j} = \frac{\omega_j}{h_{(j)}} \frac{\partial U_i}{\partial \xi_j} + \left(\omega_i U_j - U_i \omega_j\right) \kappa_{(i)j} + \frac{h_{(i)}}{h} \frac{\partial}{\partial \xi_j} \left(\frac{h}{h_{(i)}^2 h_{(j)}^2} \left(\frac{\partial}{\partial \xi_i} \left(h_{(j)} \omega_j \right) - \frac{\partial}{\partial \xi_j} \left(h_{(i)} \omega_i \right) \right) \right) \tag{A 3}$$

REFERENCES

Al-Zanaidi, M. A. & Hui, W. H. 1984 Turbulent airflow over water waves-a numerical study. *Journal of Fluid Mechanics* **148**, 225–246.

Anderson, Dale A, Tannehill, John C & Pletcher, Richard H 1984 *Computational fluid mechanics and heat transfer*, first edition edn. Hemisphere, New York.

Aris, R 1962 *Vectors, Tensors and the Basic Equations of Fluid Dynamics*. Dover New York.

Banner, Michael L. 1990 The influence of wave breaking on the surface pressure distribution in wind—wave interactions. *Journal of Fluid Mechanics* **211**, 463–495.

Banner, Michael L. & Peirson, William L. 1998 Tangential stress beneath wind-driven air–water interfaces. *Journal of Fluid Mechanics* **364**, 115–145.

Barlow, Robert S. & Johnston, James P. 1988 Structure of a turbulent boundary layer on a concave surface. *Journal of Fluid Mechanics* **191**, 137–176.

Batchelor, G K 1967 *An introduction to fluid dynamics*. Cambridge University Press.

Belcher, S. E. & Hunt, J. C. R. 1993 Turbulent shear flow over slowly moving waves. *Journal of Fluid Mechanics* **251**, 109–148.

Belcher, S. E., Newley, T. M. J. & Hunt, J. C. R. 1993 The drag on an undulating surface induced by the flow of a turbulent boundary layer. *Journal of Fluid Mechanics* **249**, 557–596.

Benjamin, T. Brooke 1959 Shearing flow over a wavy boundary. *Journal of Fluid Mechanics* **6**, 161–205.

Blin, Laurent, Hadjadj, Abdellah & Vervisch, Luc 2003 Large eddy simulation of turbulent flows in reversing systems*. *Journal of Turbulence* **4**, 1–1.

Blumberg, Alan F & Herring, H James 1987 Circulation modelling using orthogonal curvilinear coordinates. In *Elsevier oceanography series*, , vol. 45, pp. 55–88. Elsevier.

Borue, Vadim, Orszag, Steven A. & Staroselsky, Ilya 1995 Interaction of surface waves with turbulence: direct numerical simulations of turbulent open-channel flow. *Journal of Fluid Mechanics* **286**, 1–23.

Boyer, Franck & Fabrie, Pierre 2012 *Mathematical tools for the study of the incompressible Navier-Stokes equations and related models*, , vol. 183. New York, NY, USA: Springer Science & Business Media.

Bradshaw, P. 1969 The analogy between streamline curvature and buoyancy in turbulent shear flow. *Journal of Fluid Mechanics* **36**, 177–191.

Bradshaw, Peter 1973 Effects of streamline curvature on turbulent flow. *Tech. Rep.* AGARD-AG-169. Advisory Group for Aerospace Research and Development (AGARD), Neuilly Sur Seine, France.

Brown, Thomas D & Hung, Tin-Kan 1977 Computational and experimental investigations of two-dimensional nonlinear peristaltic flows. *Journal of Fluid Mechanics* **83** (2), 249–272.

Buckley, Marc P. & Veron, Fabrice 2016 Structure of the airflow above surface waves. *Journal of Physical Oceanography* **46** (5), 1377–1397.

Buckley, Marc P. & Veron, Fabrice 2017 Airflow measurements at a wavy air–water interface using piv and lif. *Experiments in Fluids* **58** (11), 161.

Buckley, M. P. & Veron, F. 2019 The turbulent airflow over wind generated surface waves. *European Journal of Mechanics - B/Fluids* **73**, 132–143.

Cebeci, Tuncer & Cousteix, Jean 2005 *Modeling and computation of boundary-layer flows*, 2nd edn. Springer-Verlag Berlin Heidelberg.

Cebeci, T, Kaups, K & Moser, A 1976 Calculation of three-dimensional boundary layers. iii-three-dimensional flows in orthogonal curvilinear coordinates. *AIAA Journal* **14** (8), 1090–1094.

Chen, HC, Patel, VC & Ju, S 1990 Solutions of reynolds-averaged navier-stokes equations for three-dimensional incompressible flows. *Journal of Computational Physics* **88** (2), 305–336.

Cheung, Tak Kee & Street, Robert L. 1988 The turbulent layer in the water at an air-water interface. *Journal of Fluid Mechanics* **194**, 133–151.

Dave, N, Azih, C & Yaras, MI 2013 A dns study on the effects of convex streamwise curvature on coherent structures in a temporally-developing turbulent boundary layer with supercritical water. *International Journal of Heat and Fluid Flow* **44**, 635–643.

Davis, Kristen A. & Monismith, Stephen G. 2011 The modification of bottom boundary layer turbulence and mixing by internal waves shoaling on a barrier reef. *Journal of Physical Oceanography* **41** (11), 2223–2241.

Degani, AT & Walker, JDA 1993 Computation of attached three-dimensional turbulent boundary layers. *Journal of Computational Physics* **109** (2), 202–214.

Druzhinin, O. A., Troitskaya, Y. I. & Zilitinkevich, S. S. 2016 Stably stratified airflow over a waved water surface. part 1: Stationary turbulence regime. *Quarterly Journal of Royal Meteorological Society* **142** (695), 759–772.

Einaudi, F & Finnigan, JJ 1993 Wave-turbulence dynamics in the stably stratified boundary layer. *Journal of the Atmospheric Sciences* **50** (13), 1841–1864.

Einaudi, F., Finnigan, J. J. & Fua, D. 1984 Gravity wave turbulence interaction in the presence of a critical level. *Journal of the Atmospheric Sciences* **41** (4), 661–667.

Elfouhaily, T, Chapron, B, Katsaros, K & Vandemark, D 1997 A unified directional spectrum for long and short wind-driven waves. *Journal of Geophysical Research: Oceans* **102** (C7), 15781–15796.

Finnigan, J. J. 1983 A streamline coordinate system for distorted two-dimensional shear flows. *Journal of Fluid Mechanics* **130**, 241–258.

Finnigan, J J 2004 A re-evaluation of long-term flux measurement techniques part ii: coordinate systems. *Boundary-Layer Meteorology* **113** (1), 1–41.

Finnigan, J. J. & Einaudi, F. 1981 The interaction between an internal gravity wave and the planetary boundary layer. part ii: Effect of the wave on the turbulence structure. *Quarterly Journal of Royal Meteorological Society* **107** (454), 807–832.

Gent, P. R. & Taylor, P. A. 1976 A numerical model of the air flow above water waves. *Journal of Fluid Mechanics* **77**, 105–128.

Grare, Laurent, Peirson, William L., Branger, Hubert, Walker, James W., Giovanangeli, Jean-Paul & Makin, Vladimir 2013 Growth and dissipation of wind-forced, deep-water waves. *Journal of Fluid Mechanics* **722**, 5–50.

Hall, Philip & Horseman, Nicola J 1991 The linear inviscid secondary instability of longitudinal vortex structures in boundary layers. *Journal of Fluid Mechanics* **232**, 357–375.

Hao, Xuanting & Shen, Lian 2019 Wind–wave coupling study using les of wind and phase-resolved simulation of nonlinear waves. *Journal of Fluid Mechanics* **874**, 391–425.

Hara, T. & Belcher, S. E. 2004 Wind profile and drag coefficient over mature ocean surface wave spectra. *Journal of Physical Oceanography* **34** (11), 2345–2358.

Hara, Tetsu & Sullivan, Peter P. 2015 Wave boundary layer turbulence over surface waves in a strongly forced condition. *Journal of Physical Oceanography* **45** (3), 868–883.

Hoffmann, PH, Muck, KC & Bradshaw, P 1985 The effect of concave surface curvature on turbulent boundary layers. *Journal of Fluid mechanics* **161**, 371–403.

Holloway, AGL, Roach, DC & Akbary, H 2005 Combined effects of favourable pressure gradient and streamline curvature on uniformly sheared turbulence. *Journal of Fluid Mechanics* **526**, 303–336.

Holloway, Arthur Gordon Lawrence & Tavoularis, S 1992 The effects of curvature on sheared turbulence. *Journal of Fluid Mechanics* **237**, 569–603.

Holloway, A. G. L. & Tavoularis, S. 1998 A geometric explanation of the effects of mild streamline curvature on the turbulence anisotropy. *Physics of Fluids* **10** (7), 1733–1741.

Hsu, Chin-Tsau & Hsu, En Yun 1983 On the structure of turbulent flow over a progressive water wave: theory and experiment in a transformed wave-following coordinate system. part 2. *Journal of Fluid Mechanics* **131**, 123–153.

Hsu, Chin-Tsau, Hsu, En Yun & Street, Robert L. 1981 On the structure of turbulent flow over a progressive water wave: theory and experiment in a transformed, wave-following co-ordinate system. *Journal of Fluid Mechanics* **105**, 87–117.

Hung, Tin-Kan & Brown, Thomas D 1977 An implicit finite-difference method for solving the navier-stokes equation using orthogonal curvilinear coordinates. *Journal of Computational Physics* **23** (4), 343–363.

Husain, Nyla T, Hara, Tetsu, Buckley, Marc P, Yousefi, Kianoosh, Veron, Fabrice & Sullivan, Peter P 2019 Boundary layer turbulence over surface waves in a strongly forced condition: LES and observation. *Journal of Physical Oceanography* **49** (8), 1997–2015.

Hussain, A. K. M. F. & Reynolds, W. C. 1970 The mechanics of an organized wave in turbulent shear flow. *Journal of Fluid Mechanics* **41**, 241–258.

Hussain, A. K. M. F. & Reynolds, W. C. 1972 The mechanics of an organized wave in turbulent shear flow. part 2. experimental results. *Journal of Fluid Mechanics* **54**, 241–261.

Iafrati, A., De Vita, F. & Verzicco, R. 2019 Effects of the wind on the breaking of modulated wave trains. *European Journal of Mechanics - B/Fluids* **73**, 6–23.

Janssen, P. A. 1989 Wave-induced stress and the drag of air flow over sea waves. *Journal of Physical Oceanography* **19** (6), 745–754.

Kantha, L H & Rosati, A 1990 The effect of curvature on turbulence in stratified fluids. *Journal of Geophysical Research: Oceans* **95** (C11), 20313–20330.

Kim, N & Rhode, DL 2000 Streamwise curvature effect on the incompressible turbulent mean velocity over curved surfaces. *Journal of fluids engineering* **122** (3), 547–551.

Kundu, Pijush K. & Cohen, Ira M. 2002 *Fluid Mechanics*, 2nd edn. Academic Press.

Longuet-Higgins, Michael S. 1969 Action of a variable stress at the surface of water waves. *Physics of Fluids* **12** (4), 737–740.

Longuet-Higgins, Michael S. 1998 Vorticity and curvature at a free surface. *Journal of Fluid Mechanics* **356**, 149–153.

Lumley, J. L. & Terray, E. A. 1983 Kinematics of turbulence convected by a random wave field. *Journal of Physical Oceanography* **13** (11), 2000–2007.

Makin, VK & Kudryavtsev, VN 2002 Impact of dominant waves on sea drag. *Boundary-Layer Meteorology* **103** (1), 83–99.

Makin, V. K. & Kudryavtsev, V. N. 1999 Coupled sea surface-atmosphere model: 1. wind over waves coupling. *Journal of Geophysical Research: Oceans* **104** (C4), 7613–7623.

Makin, V. K., Kudryavtsev, V. N. & Mastenbroek, C. 1995 Drag of the sea surface. *Boundary-Layer Meteorology* **73** (1-2), 159–182.

Makin, V. K. & Mastenbroek, C. 1996 Impact of waves on air-sea exchange of sensible heat and momentum. *Boundary-Layer Meteorology* **79** (3), 279–300.

Mastenbroek, C., Makin, V. K., Garat, M. H. & Giovanangeli, J. P. 1996 Experimental evidence of the rapid distortion of turbulence in the air flow over water waves. *Journal of Fluid Mechanics* **318**, 273–302.

Moser, Robert D & Moin, Parviz 1987 The effects of curvature in wall-bounded turbulent flows. *Journal of Fluid Mechanics* **175**, 479–510.

Mueller, J A & Veron, F 2009 Nonlinear formulation of the bulk surface stress over breaking waves: feedback mechanisms from air-flow separation. *Boundary-Layer Meteorology* **130** (1), 117–134.

Náraigh, Lennon Ó, Spelt, Peter DM & Zaki, Tamer A 2011 Turbulent flow over a liquid layer revisited: multi-equation turbulence modelling. *Journal of Fluid Mechanics* **683**, 357–394.

Nash, John F. & Patel, Virendra C. 1972 *Three-Dimensional Turbulent Boundary Layers*. Atlanta, GA: Scientific and Business Consultants Inc.

Neves, João C, Moin, Parviz & Moser, Robert D 1994 Effects of convex transverse curvature on wall-bounded turbulence. part 1. the velocity and vorticity. *Journal of Fluid Mechanics* **272**, 349–382.

Nikitin, Nikolay 2006 Finite-difference method for incompressible navier–stokes equations in arbitrary orthogonal curvilinear coordinates. *Journal of Computational Physics* **217** (2), 759–781.

Nikitin, Nikolay 2011 Four-dimensional turbulence in a plane channel. *Journal of Fluid Mechanics* **680**, 67–79.

Nikitin, Nikolay, Wang, Hengliang & Chernyshenko, Sergei 2009 Turbulent flow and heat transfer in eccentric annulus. *Journal of Fluid Mechanics* **638**, 95–116.

Raithby, GD, Galpin, PF & Van Doormaal, JP 1986 Prediction of heat and fluid flow in complex geometries using general orthogonal coordinates. *Numerical Heat Transfer, Part A: Applications* **9** (2), 125–142.

Ramaprian, BR & Shivaprasad, BG 1978 The structure of turbulent boundary layers along mildly curved surfaces. *Journal of Fluid Mechanics* **85** (2), 273–303.

Ramaprian, BR & Shivaprasad, BG 1982 The instantaneous structure of mildly curved turbulent boundary layers. *Journal of Fluid Mechanics* **115**, 39–58.

Redzic, Dragan V 2001 The operator ∇ in orthogonal curvilinear coordinates. *European Journal of Physics* **22** (6), 595.

Reynolds, W. C. & Hussain, A. K. M. F. 1972 The mechanics of an organized wave in turbulent shear

flow. part 3. theoretical models and comparisons with experiments. *Journal of Fluid Mechanics* **54**, 263–288.

Richmond, MC, Chen, HC & Patel, Virendrakumar Chaturbhai 1986 Equations of laminar and turbulent flows in general curvilinear coordinates. Technical report No. IIHR-300. Iowa Institute of Hydraulic Research, Iowa, USA.

Rutgersson, A. & Sullivan, P. P. 2005 The effect of idealized water waves on the turbulence structure and kinetic energy budgets in the overlying airflow. *Dynamics of Atmospheres and Oceans* **38** (3-4), 147–171.

Shen, Luyu, Lu, Changgen, Wu, Weiguo & Xue, Shifeng 2015 A high-order numerical method to study three-dimensional hydrodynamics in a natural river. *Advances in Applied Mathematics and Mechanics* **7** (2), 180–195.

Shen, Lian, Zhang, Xiang, Yue, Dick K. P. & Triantafyllou, Michael S. 2003 Turbulent flow over a flexible wall undergoing a streamwise travelling wave motion. *Journal of Fluid Mechanics* **484**, 197–221.

Shikhmurzaev, Yulii D & Sisoev, Grigori M 2017 Spiralling liquid jets: verifiable mathematical framework, trajectories and peristaltic waves. *Journal of Fluid Mechanics* **819**, 352–400.

Shyu, Jinn-Hwa & Phillips, O M 1990 The blockage of gravity and capillary waves by longer waves and currents. *Journal of Fluid Mechanics* **217**, 115–141.

So, Ronald MC 1975 A turbulence velocity scale for curved shear flows. *Journal of Fluid Mechanics* **70** (1), 37–57.

So, Ronald MC & Mellor, George L 1973 Experiment on convex curvature effects in turbulent boundary layers. *Journal of Fluid Mechanics* **60**, 43–62.

Sullivan, Peter P., Banner, Michael L., Morison, Russel P. & Peirson, William L. 2018 Turbulent flow over steep steady and unsteady waves under strong wind forcing. *Journal of Physical Oceanography* **48** (1), 3–27.

Sullivan, Peter P., Edson, James B., Hristov, Tihomir & McWilliams, James C. 2008 Large-eddy simulations and observations of atmospheric marine boundary layers above nonequilibrium surface waves. *Journal of the Atmospheric Sciences* **65** (4), 1225–1245.

Sullivan, Peter P., McWilliams, James C. & Moeng, Chin-Hoh 2000 Simulation of turbulent flow over idealized water waves. *Journal of Fluid Mechanics* **404**, 47–85.

Sullivan, Peter P., McWilliams, James C. & Patton, Edward G. 2014 Large-eddy simulation of marine atmospheric boundary layers above a spectrum of moving waves. *Journal of the Atmospheric Sciences* **71** (11), 4001–4027.

Takeuchi, K., Leavitt, E. & Chao, S. P. 1977 Effects of water waves on the structure of turbulent shear flow. *Journal of Fluid Mechanics* **80**, 535–559.

Thais, Laurent & Magnaudet, Jacques 1995 A triple decomposition of the fluctuating motion below laboratory wind water waves. *Journal of Geophysical Research: Oceans* **100** (C1), 741–755.

Townsend, A A 1972 Flow in a deep turbulent boundary layer over a surface distorted by water waves. *Journal of Fluid Mechanics* **55** (4), 719–735.

Tsai, Wu-ting, Chen, Shi-ming & Lu, Guan-hung 2015 Numerical evidence of turbulence generated by nonbreaking surface waves. *Journal of Physical Oceanography* **45** (1), 174–180.

Tseluiko, Dmitri & Kalliadasis, Serafim 2011 Nonlinear waves in counter-current gas–liquid film flow. *Journal of Fluid Mechanics* **673**, 19–59.

Veron, F., Saxena, G. & Misra, S. K. 2007 Measurements of the viscous tangential stress in the airflow above wind waves. *Geophysical Research Letters* **34** (19).

Vinokur, Marcel 1974 Conservation equations of gasdynamics in curvilinear coordinate systems. *Journal of Computational Physics* **14** (2), 105–125.

Xuan, Anqing, Deng, Bing-Qing & Shen, Lian 2019 Study of wave effect on vorticity in langmuir turbulence using wave-phase-resolved large-eddy simulation. *Journal of Fluid Mechanics* **875**, 173–224.

Yang, Di & Shen, Lian 2017 Direct numerical simulation of scalar transport in turbulent flows over progressive surface waves. *Journal of Fluid Mechanics* **819**, 58–103.

Yang, D. I. & Shen, Lian 2010 Direct-simulation-based study of turbulent flow over various waving boundaries. *Journal of Fluid Mechanics* **650**, 131–180.

Yang, Zixuan, Deng, Bing-Qing & Shen, Lian 2018 Direct numerical simulation of wind turbulence over breaking waves. *Journal of Fluid Mechanics* **850**, 120–155.

Yousefi, Kianoosh, Veron, Fabrice & Buckley, Marc P. 2019 Momentum flux measurements in the airflow over wind-generated surface waves. *Journal of Fluid Mechanics*, Under Review.

Zhao, D. & Toba, Y. 2001 Dependence of whitecap coverage on wind and wind-wave properties. *Journal of Oceanography* **57** (5), 603–616.

Boundary layer formulations in orthogonal curvilinear coordinates for flow over wind-generated surface waves

Journal of Fluid Mechanics, Volume 888

DOI: 10.1017/jfm.2020.32

Published online: 06 February 2020

Print publication: April 2020

Summary

The development of the governing equations for fluid flow in a surface-following coordinate system is essential to investigate the fluid flow near an interface deformed by propagating waves. In this paper, the governing equations of fluid flow, including conservation of mass, momentum and energy balance, are derived in an orthogonal curvilinear coordinate system relevant to surface water waves. All equations are further decomposed to extract mean, wave-induced and turbulent components. The complete transformed equations include explicit extra geometric terms. For example, turbulent stress and production terms include the effects of coordinate curvature on the structure of fluid flow. Furthermore, the governing equations of motion were further simplified by considering the flow over periodic quasi-linear surface waves wherein the wavelength of the disturbance is large compared to the wave amplitude. The quasi-linear analysis is employed to express the boundary layer equations in the orthogonal wave-following curvilinear coordinates with the corresponding decomposed equations for the mean, wave and turbulent fields. Finally, the vorticity equations are also derived in the orthogonal curvilinear coordinates in order to express the corresponding velocity–vorticity formulations. The equations developed in this paper proved to be useful in the analysis and interpretation of experimental data of fluid flow over wind-generated surface waves. Experimental results are presented in a companion paper.